Chicken Skeletal Muscle Ryanodine Receptor Isoforms: Ion Channel Properties

Ann L. Percival,* Alan J. Williams,§ James L. Kenyon,‡ Matthew M. Grinsell,* Judith A. Airey,* and John L. Sutko*

Departments of *Pharmacology and ‡Physiology, University of Nevada School of Medicine, Reno, Nevada 89557 USA, and §Department of Cardiac Medicine, National Heart & Lung Institute, University of London, London SW3 6LY, England

ABSTRACT To define the roles of the α- and β-ryanodine receptor (RyR) (sarcoplasmic reticulum Ca^{2+} release channel) isoforms expressed in chicken skeletal muscles, we investigated the ion channel properties of these proteins in lipid bilayers. α- and βRyRs embody Ca^{2+} channels with similar conductances (792, 453, and 118 pS for K^+, Cs^+, and Ca^{2+}) and selectivities ($P_{Ca^{2+}}/P_{K^+}$ = 7.4), but the two channels have different gating properties. αRyR channels switch between two gating modes, which differ in the extent they are activated by Ca^{2+} and ATP, and inactivated by Ca^{2+}. Either mode can be assumed in a spontaneous and stable manner. In a low activity mode, αRyR channels exhibit brief openings (τ_o = 0.14 ms) and are minimally activated by Ca^{2+} in the absence of ATP. In a high activity mode, openings are longer (τ_{o1-3} = 0.17, 0.51, and 1.27 ms), and the channels are activated by Ca^{2+} in the absence of ATP and are in general less sensitive to the inactivating effects of Ca^{2+}. βRyR channel openings are longer (τ_{o1-3} = 0.34, 1.56, and 3.31 ms) than those of αRyR channels in either mode. βRyR channels are activated to a greater relative extent by Ca^{2+} than ATP and are inactivated by millimolar Ca^{2+} in the absence, but not the presence, of ATP. Both α- and βRyR channels are activated by caffeine, inhibited by Mg^{2+} and ruthenium red, inactivated by voltage (cytoplasmic side positive), and modified to a long-lived substate by ryanodine, but only αRyR channels are activated by perchlorate anions. The differences in gating and responses to channel modifiers may give the α- and βRyRs distinct roles in muscle activation.

INTRODUCTION

As sarcoplasmic reticulum (SR) Ca^{2+} release channels (Campbell et al., 1987; Inui et al., 1987; Lai et al., 1988; Smith et al., 1988), the ryanodine receptors (RyR) participate in coupling cellular excitation to SR Ca^{2+} release and contraction in striated muscles. Two mechanisms have been proposed to activate RyR channels in skeletal muscle. One involves either direct or indirect interactions between dihydropyridine receptors and RyRs, whereas in the second mechanism RyR channels are activated by Ca^{2+} released from the SR (for references, see Rios and Pizarro, 1988, 1991; Jacquemond et al., 1991). Once released, SR Ca^{2+} may also inactivate the RyR channel (Simon et al., 1991; Hollingworth et al., 1992), and the net consequence of the activating and inactivating effects of this cation is at present unclear (Pape et al., 1993; Jong et al., 1993).

Excitation-contraction coupling is thought to be similar in mammalian and nonmammalian vertebrate skeletal muscles. Moreover, frog skeletal muscles are commonly used to study this process. Two RyRs are co-expressed in a number of avian, amphibian, and piscine fast twitch skeletal muscles (Airey et al., 1990; Olivares et al., 1991; Lai et al., 1992; Murayama and Ogawa, 1992; O'Brien et al., 1993), while only a single receptor protein has been identified to date in mammalian skeletal muscle (Campbell et al., 1987; Inui et al., 1987; Lai et al., 1988). This raises the question of whether the properties of the two RyRs found in nonmammalian vertebrate muscles have been combined in the single mammalian skeletal muscle RyR to provide the same functional capabilities. For example, each of the nonmammalian skeletal muscle RyR isoforms could be adapted to be activated by a different mechanism. Alternatively, an as yet undetected ryanodine receptor isoform may be expressed in mammalian muscle. In this regard, Giannini et al. (1992) presented evidence for the expression of the brain RyR isoform (RyR3) in mammalian skeletal muscle. A third possibility is that there may be differences between the excitation-contraction in mammalian and nonmammalian vertebrate muscles.

Several observations indicate that the two ryanodine receptor isoforms (α and β) expressed in chicken skeletal muscles are distinct proteins with different roles in both embryonic and mature muscles. First, biochemically these isoforms differ in their molecular mass as judged from their mobilities on SDS gels, in their susceptibility to proteolysis by trypsin, and in the peptide maps generated by proteolytic digestion (Airey et al., 1990, 1993c). Second, they differ immunologically, because monoclonal antibodies recognize unique as well as shared epitopes in each isoform (Airey et al., 1993c). Third, they may be regulated differently, because they are phosphorylated by the Ca^{2+}, calmodulin-dependent and the cAMP-dependent protein kinases ($\beta \gg \alpha$), and bind calmodulin ($\alpha > \beta$) to different extents (Airey et al., 1993c). Fourth, the α- and βRyRs differ as to the timing of their initial expression in embryonic muscles. The αRyR is found in peripheral muscles at ~day E6, whereas βRyR cannot be detected until ~day E18 (Sutko et al., 1991;

Received for publication 10 May 1994 and in final form 5 August 1994.

Address reprint requests to John L. Sutko, Department of Pharmacology/318, University of Nevada School of Medicine, Reno, NV 89557. Tel.: 702-784-4121; Fax: 702-784-1620; E-mail: sutko@pognip.unr.edu.

0006-3495/94/11/1834/17 $2.00

M. D. Baring, J. A. Airey, and J. L. Sutko, unpublished observations). Fifth, both RyRs are expressed in mature muscles (Airey et al., 1990), indicating that although a single isoform may be transiently sufficient in developing muscle, two receptors are required for mature muscle function. Sixth, the *Crooked Neck Dwarf* (cn) mutation in chickens is associated with a failure to make normal αRyR. Although cultured embryonic cn/cn skeletal muscle cells have normal levels of a functional βRyR, they are dysgenic, fail to form normal sarcomeres, and undergo a degenerative cell death indicating a requirement for an αRyR-specific function for normal muscle development (Airey et al., 1993a, b).

Although the preceding data indicate that the two chicken skeletal muscle RyR isoforms are unique proteins, they do not address directly their potential as SR Ca^{2+} release channels. Therefore, we investigated the ion channel characteristics of these proteins to gain insight into how each isoform may contribute to muscle activation. Our results indicate that although both isoforms embody ion channels with similar conductance and selectivity properties, they differ in their gating behaviors and responses to channel modifiers. These results provide direct evidence that the α- and βRyR SR Ca^{2+} release channels have the potential to serve distinct roles in excitation-contraction coupling in chicken skeletal muscles.

MATERIALS AND METHODS

Materials

Fertile White Leghorn eggs were purchased from Western Scientific (Rio Linda, CA). Leupeptin, piperazine-*N*,*N*′-bis[2-ethanesulfonic acid] (PIPES), tris[hydroxymethyl]aminomethane (Tris), *N*-[2-hydroxyethyl]-piperazine-*N*′-[2-ethanesulfonic acid] (HEPES), imidazole, phenylmethylsulfonylfluoride (PMSF), 3-[(3-cholamidopropyl)-dimethylammonio]-1-propanesulfonate (CHAPS), L-α-phosphatidylcholine (PC, for ryanodine receptor solubilization), agarose-linked goat anti-mouse immunoglobulin (IgG, whole molecule) antibodies, polyethylenimine (PEI), ethylene glycolbis(β-aminoethylether)-*N*,*N*,*N*′,*N*′-tetraacetic acid (EGTA), *N*-hydroxyethylethylenediamine triacetic acid (HEDTA), triton X-100, adenosine triphosphate (ATP, sodium salt), caffeine, and ruthenium red were purchased from Sigma Chemical Co. (St. Louis, MO). Dithiothreitol (DTT) was from Boehringer Mannheim Biochemicals (Indianapolis, IN). Alkaline phosphatase-conjugated goat anti-mouse IgG was from Fisher (San Francisco, CA). Sodium dodecyl sulfate polyacrylamide gel electrophoresis (SDS-PAGE) molecular weight standards were from Bio-Rad Laboratories (Richmond, CA), and the L-α-PC, L-α-phosphatidylethanolamine (PE), and L-α-phosphatidylserine (PS) used for the bilayer studies were from Avanti Polar Lipids (Alabaster, AL).

The hybridoma, MF20, developed by Dr. D. Fischman (Cornell University, Ithaca, NY) was obtained from the Developmental Studies Hybridoma Bank maintained by the Department of Pharmacology and Molecular Sciences, The Johns Hopkins University School of Medicine (Baltimore, MD) and the Department of Biology, University of Iowa (Iowa City, IA) under contract NO1-HD-2-3144 from the NICHD.

Membrane preparation and RyR purification

Microsomal membranes and membranes enriched in SR terminal cisternae were prepared from chicken pectoral muscle as described previously (Airey et al., 1990) and resuspended in 10 mM imidazole, 0.5 M sucrose. These membranes were used for both bilayer experiments and for the preparation of purified RyRs. Proteins were differentially extracted from these membranes with 2% triton X-100 followed by solubilization of the RyRs with CHAPS (1.0%) in the presence of 0.5% PC (Airey et al., 1990). Solubilized and nonsolubilized materials were separated by centrifugation at 100,000 × *g* for 30 min. α- and βRyRs were purified by sedimentation through continuous 10–30% sucrose gradients containing 0.5% CHAPS, 0.25% PC, and separated by selectively depleting one of the isoforms using isoform-specific monoclonal antibodies (Mabs, 5D4 = anti-αRyR; 110E = anti-βRyR). In some cases, the individual RyRs were purified further by sedimentation through a second sucrose gradient. In control experiments to demonstrate that the observed channel activity was associated with the RyR isoforms, both RyRs were depleted using a third antibody (34C) that recognizes an epitope common to both isoforms. Membrane and purified proteins were quantitated using the method of Lowry et al. (1951), as modified by Peterson (1977). Murayama and Ogawa (1992) found that the inclusion of DTT stabilized the ion channel activity of the frog RyRs. Based on this observation, we included 5 mM DTT in our purified RyR preparations. We did not investigate the effectiveness of this agent in detail, but it is our impression that αRyR channel activity was more stable in the presence of DTT.

Planar lipid bilayer experiments

RyR single-channel experiments were performed using the paradigms developed by Smith et al. (1985, 1986) and Rousseau et al. (1987). Mueller-Rudin type bilayers were painted across a 200 μm hole in a polystyrene cup using a 5:3:2 mixture of PE:PS:PC (50 mg/ml in decane). In studies utilizing purified RyRs, a solution containing 210 mM KCl, 50 mM HEPES (pH 7.4), 1 mM EGTA, 1 mM HEDTA, and 10 μM free Ca^{2+} was added to the *cis* and *trans* chambers, 300–600 mM KCl was added to the *cis* chamber to create an ionic gradient across the bilayer, and 0.1–0.5 μg of receptor protein was added to the *cis* chamber. After incorporation of a channel into the bilayer, the *cis* chamber was perfused with 7–10 volumes of a solution containing 210 mM KCl, 50 mM HEPES (pH 7.4), 1 mM EGTA, 1 mM HEDTA, and 0.3 μM free Ca^{2+} to prevent any further RyR incorporation and to set the *cis* Ca^{2+} initially to a low level. NaCl was substituted for KCl in experiments where the actions of perchlorate were investigated because of the greater solubility of the sodium salt of this anion. For experiments using SR terminal cisternae membranes, a solution containing 210 mM CsPIPES (pH 7.4), 1 mM EGTA, and 10 μM free Ca^{2+} was added to both the *cis* and *trans* chambers, an ionic gradient was created across the bilayer by the addition of 300 mM KCl to the *cis* chamber, and 5–15 μg of membrane protein were added to the *cis* chamber. After vesicle fusion with the bilayer, the *cis* chamber was perfused with 7–10 volumes of a solution containing 210 mM CsPIPES (pH 7.4), 1 mM EGTA, and 0.3 μM free Ca^{2+}. Solutions were passed through 0.22 μm filters before use, and RyR channel modifiers were added as described in Results for individual experiments. In the present studies, the orientation of RyR channels in the bilayer was such that the cytoplasmic domain of the receptor was on the *cis* side of the bilayer. This was confirmed by assessing the abilities of Ca^{2+} and ATP added to either the *cis* or *trans* chambers to activate the channels.

In experiments where the effects of a complete range of free Ca^{2+} levels was investigated, a combination of EGTA (1 mM) and HEDTA (1 mM) was used to provide control over a wide range of Ca^{2+} concentrations. EGTA (1 mM) alone was used when micromolar and submicromolar Ca^{2+} concentrations were desired. Free Ca^{2+} levels obtained with the HEDTA/EGTA system were calculated using the program Frion (from Dr. Noel Davies, University of Leicester), whereas those obtained with the EGTA system were defined using the program Iterate (from Dr. Robert Godt, Medical College of Georgia). Free Ca^{2+} levels were verified in control experiments using a Ca^{2+}-sensitive electrode (Radiometer, Cophenhagen, Denmark).

Single-channel currents were recorded using a bilayer/amplifier system designed by R. A. P. Montgomery (University of London), stored unfiltered on videotape, and then filtered using 8-pole low pass Bessel filter (Frequency Devices, Haverhill, MA) at 3–5 kHz before digitization at 16 kHz. Voltages were applied to the *cis* side of the bilayer, whereas the *trans* side was held at virtual ground. Channel openings associated with outward currents (cytosol to SR lumen, or *cis* to *trans*) are downward deflections, whereas those associated with inward currents (SR lumen to cytosol, or *trans* to *cis*) are upward. Because of the wide range of the levels of activation observed for the chicken RyR isoform channels in these studies, current

records 6 min in length were utilized for analysis to ensure that accurate estimates of channel parameters were obtained.

Digitization and analysis were accomplished using pClamp hardware and software and IPROC software (Axon Instruments, Foster City, CA). Curve fitting and graphical presentation were accomplished using Sigma Plot software (v. 4.1, Corte Madera, CA). Openings were identified using a 50% threshold. Amplitude histograms were obtained as all-points histograms using a 0.5 pA bin size. Mean P_o values were calculated for 6 min records using the stationarity file generated by the IPROC software with P_o values determined every 100 or 128 ms intervals and averaged for 6 min records. The relative permeabilities of Ca^{2+} and K^+ ($P_{Ca^{2+}}/P_{K^+}$) were calculated from the reversal potential obtained under the biionic conditions shown in Fig. 3 using Eq. 1 of Fatt and Ginsborg (1958). The concentrations of Ca^{2+} yielding half-maximal activation or inhibition of channel activity were determined graphically.

Dwell-time histograms were fit using the nonlinear regression curve-fitting routine in Sigma Plot, which is based on the Marquardt-Levenberg algorithm. The goodness of a fit of curves generated by equations with differing numbers of exponentials was evaluated using three criteria: (i) the adequacy of the total fit of the curve to the histogram as judged by eye, (ii) the norm and dependency values associated with the different fits that are available from the Sigma Plot routine, and (iii) the failure of inclusion of additional exponential terms to produce a meaningful change in the derived time constants. The mean open and closed channel lifetimes reported in Table 3 and shown in Fig. 7 were calculated using the time constant and area% values derived from the dwell-time histograms. The probability density functions (pdfs) shown in Fig. 7 *E* have units of s^{-1} and were calculated by dividing the number of events in each bin of dwell-time histograms by the total area under the curve fit to the dwell-time histogram (Colquhoun and Sigworth, 1983). Mean channel lifetimes are reported to give insights into the net changes in channel gating behavior under different activating conditions, whereas the pdfs are provided to illustrate the shifts in the open and closed event lifetimes under these conditions.

The shortest event that was fully resolved by our bilayer system was 100 μs. Openings shorter than 150 μs were not included in analyses of channel lifetimes. Extrapolations of the exponential curves fit to the dwell-time histograms of fully resolved events suggested that there were many openings by αRyR channels in particular, but by βRyR channels as well, that were shorter than the dead time of the bilayer system. This was especially true in the absence of ATP. The presence of these events is also indicated by a large number of truncated openings in the current records and amplitude histograms (Fig. 2). Parameters derived from the dwell-time histograms have not been corrected for missed events; they are intended to describe the characteristics of the events that were fully resolved by our bilayer. It should also be noted that not all of the channels analyzed exhibited each of the time constants described in Tables 1 and 2. The means (±SEM) given for time constants and the area-% values given for a particular channel type may therefore be derived from different numbers of observations. The area-% values indicate the proportion of the total number of openings or closings represented by a particular time constant in only the channels that exhibited that time constant. Therefore, in cases where not all of the channels analyzed had each of the time constants, the sum of the area-% values for the time constants observed for that channel type do not equal 100%. Data described in the text are given as means ± SEM.

RESULTS

The objectives of these studies were to determine whether the RyR isoforms expressed in chicken skeletal muscles embody ion channels and, if so, to define their basic properties. The α- and βRyRs co-exist in the same muscle fibers; therefore, to define the properties of each protein unambiguously it was necessary to purify each isoform. This was accomplished using isoform-specific Mabs to precipitate and remove one of the isoforms leaving the other in solution. The latter RyR was studied, thus eliminating the need for the harsh treatments required to recover proteins from antibody-antigen complexes. A RyR preparation typical of those utilized in some of our studies is shown in Fig. 1. In most preparations, only RyR subunit polypeptides (*arrowheads*) and polypeptides that migrated just ahead of the subunit polypeptides (shown by Western analysis to be derived from the RyR subunits) were evident in SDS gels stained for protein with Coomassie Brilliant Blue. The latter polypeptides derived from the αRyR (Fig. 1, *lane* 2) and that derived from the βRyR (Fig. 1, *lane* 3) had different mobilities. Occasionally the myosin heavy chain (indicated by the *filled circle* in Fig.1) and an approximately 66 kDa polypeptide derived from the secondary antibody preparations (indicated by the *asterisk*) were also present. In some of these preparations, myosin was removed by including an anti-myosin Mab (MF20) in the precipitation step and the antibody-related peptide was deleted by sedimentation through a second sucrose gradient. Removal of these non-RyR proteins did not alter the channel activity observed. To demonstrate further that the channel activities observed were attributable to α- and βRyRs, the Mab 34C, which recognizes both isoforms, was used to deplete the α- and βRyRs (Fig. 1, *lane* 4). No channel activity was observed in these preparations (data not shown).

As described below, the ion channels that incorporated into bilayers from α- and βRyR preparations exhibited dis-

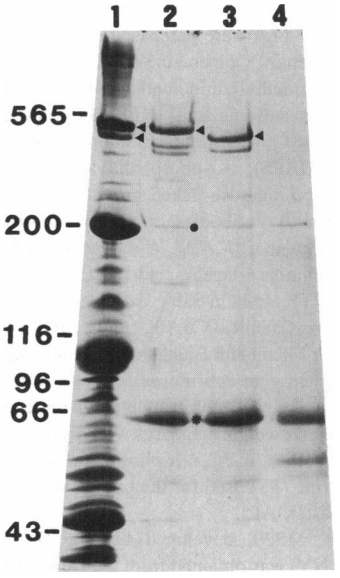

FIGURE 1 SDS-polyacrylamide gel showing typical partially purified α (*lane* 2) and βRyR (*lane* 3) preparations used for a majority of the experiments described in this report. The SR membranes from which these proteins were isolated (*lane* 1) and a RyR receptor preparation depleted of both the α and β isoforms (*lane* 4) are also shown. The α- and βRyR subunit polypeptides are indicated by the arrowheads in lanes 1–3, the polypeptide at 200 kDa indicated by the circle in lane 2 is the heavy chain of myosin; the approximately 66 kDa polypeptide indicated by the asterisk in Lane 2 was derived from the antibody preparation used in the precipitation step. Elimination of either myosin or the antibody polypeptides by further purification steps did not alter the RyR channel activity observed. The other minor bands seen in Lanes 2 and 3 represent RyR breakdown products. No ion channel activity was observed when both RyR isoforms were depleted (*lane* 4).

tinctive gating behaviors. Channels with properties we attribute to αRyRs were observed for 76 of 86 (88.4%) channels analyzed from αRyR preparations, whereas channels typified as βRyR were obtained for 10 channels from the αRyR preparation and for 64 of 64 (100%) channels analyzed from βRyR preparations. It is our impression from a large number of experiments that βRyR channels incorporate into bilayers much more readily than αRyR channels. This may explain why βRyR channels were occasionally obtained from αRyR preparations even though contaminating βRyR protein was not detectable on protein-stained SDS gels or by Western analysis. Based on the relative purification of the two isoforms achieved, the number of fusions analyzed, and the frequency that each channel type was obtained from each RyR preparation, we have assigned the characteristics observed in the majority of the studies with each preparation as being representative of that isoform. The clear cut and consistent differences observed in the gating behaviors of each channel type and the fact that the channel type identified as the βRyR was seen in 100% of the βRyR preparations strongly support this assignment. The results presented were obtained using six separate α- and βRyR preparations.

Purified RyRs: conductance characteristics

The chicken α- and βRyR ion channels have similar single-channel current amplitudes. As shown in Fig. 2, single current amplitudes of 28.3 ± 0.6 (n = 7) and 28.0 ± 0.5 pA (n = 7) were observed for α- and βRyR channels in symmetrical 210 mM KCl at a voltage of −40 mV. Well resolved openings by either α- or βRyR channels to subconductance states were rare and did not make a noticeable contribution to the distribution of current amplitudes (Fig. 2). A significant number of events that were too brief to be completely resolved were present in records obtained for both channel types, particularly the αRyR channel. These brief openings are responsible for the events accumulated between 5 and 25 pA in Fig. 2.

Current-voltage relationships recorded in symmetrical 210 mM K^+ for α- and βRyR channels were linear and had similar slope conductances of 771 ± 11.2 pS (n = 5) and 795 ± 16.4 pS (n = 3) when channels were activated by contaminating (1–3 μM) *cis* Ca^{2+} (Fig. 3). A conductance of 453 pS was observed in symmetrical 210 mM CsPIPES, and one of 118 pS was obtained for *trans* 55 mM $CaCl_2$ (measured over −10 to −110 mV) under biionic conditions with 125 mM Tris as the charge carrier on the *cis* side (data not shown). Both channels were selective for divalent over monovalent cations with $P_{Ca^{2+}}/P_{K^+}$ ratio of 7.4 (Fig. 3). These findings indicate that the α- and βRyR channels have similar conduction pathways.

Purified RyRs: open probabilities and gating behavior

In 30 μM (*cis*) activating Ca^{2+}, βRyR channels had greater open probabilities (P_o) than αRyR channels. The mean P_o values defined for the α and β channels of 0.26 and 0.71 are significantly different ($p < 0.05$). αRyR channels were activated to a relatively greater extent by 5 mM ATP + 30 μM Ca^{2+} than were βRyR channels (Fig. 4 *A*). In addition, αRyR channels exhibited a greater range of P_o values (14-fold) when activated by 30 μM (*cis*) Ca^{2+} than did βRyR channels (2.2-fold). As shown in Fig. 4, *B* and *D*, this variability is due at least in part to the ability of αRyR channels to assume two gating modes having different P_o values.

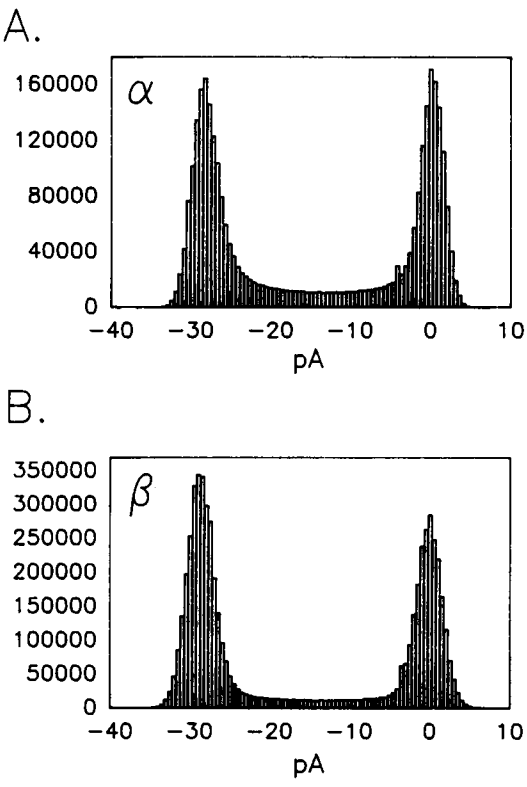

FIGURE 2 Amplitude histograms showing the distributions of the single-channel current amplitudes recorded for purified α (α_H) (*A*) and β (*B*) RyR channels. The current records utilized for this analysis were recorded at −40 mV (*cis* negative) in symmetrical 210 mM K^+ in the presence of either 50 (α) or 30 (β) μM *cis* Ca^{2+}. Under these conditions, the α and β channels had P_o values of 0.58 and 0.67, respectively.

The αRyR shown in Fig. 4, *B* and *D* switched spontaneously and reversibly between gating modes having relatively low (0.20) and high (0.87) P_o values. α channels exhibited either gating mode in a stable manner (e.g., for minutes at a time) and in 15 of 20 experiments conducted in a way that permitted the different modes to be distinguished, only a single mode was observed. In the remaining five experiments, α channels were observed to switch between modes. Using the mean P_o value shown in Fig. 4 *A* to separate channels into low and high activity modes, it can be appreciated that we observed roughly comparable numbers of channels in each gating mode. Because of their ability to switch between modes, αRyR channels are capable of quite different behaviors and, as described below, the extent these channels are activated by ATP and activated as well as inactivated by Ca^{2+} is also dependent on the gating mode they assume. The

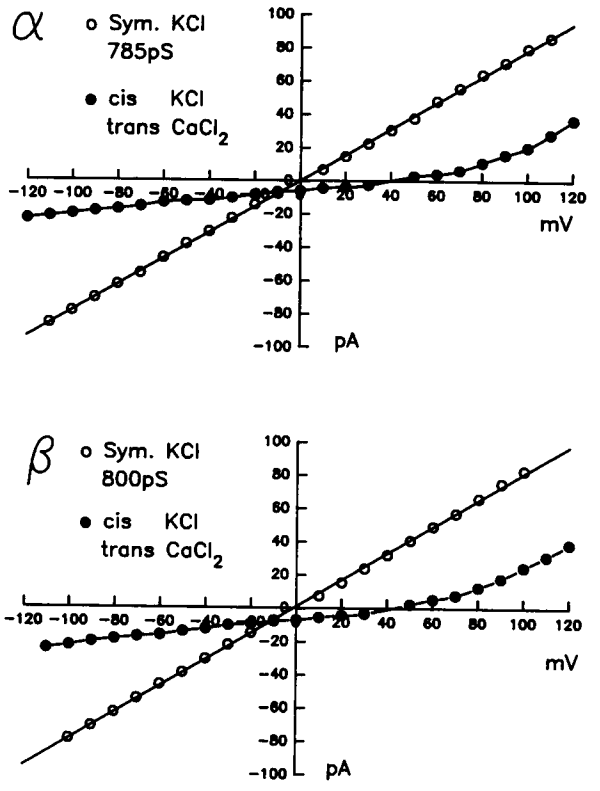

FIGURE 3 Single-channel current-voltage relationships for purified α (*top*) and βRyR (*bottom*) channels recorded in symmetrical 210 mM KCl (○), or in 210 mM KCl (*cis*), and or in 210 mM $CaCl_2$ (*trans*) (●).

possibility of unpredictable changes in channel activity added a degree of uncertainty to determinations of P_o. To minimize this potential complication, 6 min records during which a constant activity pattern was observed were used for most analyses. In cases where the mode status of the channel was in question, differences in the relative responses to 30 μM Ca^{2+} ± 5 mM ATP were used to identify the gating mode of the channel (e.g., compare Fig. 7, *A* and *B*).

As shown in Table 1 and Fig. 5, the majority of αRyR channel openings were extremely brief and the increased P_o values observed for the high activity gating mode were associated with the appearance of longer channel openings. In the low activity mode (α_L, Fig. 5 *A*), extremely short-lived events (τ_{o1} = 0.14, Table 1) accounted for 92% of the observed openings. Moreover, all of the openings of 5 of the 11 channels in this group were described by this single time constant (Table 1). In the high activity mode (α_H, Fig. 5 *B*), a significant number of longer events described by time constants of τ_{o2} = 0.51 ms and τ_{o3} = 1.27 ms accounted for 39 and 18% of the observed openings, respectively. The third time constant (τ_{o3}) was only observed for α channels in the high activity mode and may represent a conformation specific to this mode. All six channels in the α_H group exhibited three open time constants (Table 1). In parallel with the increase in open channel lifetimes, the predominant closed times associated with the high activity state were shorter than those observed for channels in the low activity mode (Table 2). As noted previously, a large number of αRyR channel openings were too brief to be completely resolved because of the frequency response of the bilayer system. Given this limitation, the τ_{o1} value obtained for this channel must be considered an upper estimate.

The most numerous openings by βRyR channels were longer than those observed for αRyR channels in either activity mode (Fig. 5 *C* and Table 1). Time constants of 1.56 (τ_{o2}) and 3.31 (τ_{o3}) ms were representative of 63 and 34% of the observed openings, respectively. When a bin size of 0.05 ms was used for the dwell-time histograms, a significant number of longer openings appeared in the last bin and were excluded from the analysis. Using a bin size of 0.5 ms, the longest time constant (τ_{o3}) was found to be 3.96 ms (Fig. 5 *D* and Table 1), which is similar to the largest τ obtained with a 0.05 ms bin size. βRyR channels also underwent transitions between different levels of activation, but these were much more rapid than those observed for the αRyR channel (Fig. 4, *C* and *E*). Thus, in contrast to the αRyR channel, which is typified by short, spike-like openings, the predominant βRyR channel openings are longer (Table 1 and Fig. 4, *D* and *E*). The differences between the open time constants that typified α- and βRyR channels remained significant when the two channel types had comparable P_o values. Moreover, the length of channel openings, particularly in low activating Ca^{2+}, could be used to identify each channel type (e.g., compare the current records for a pCa of 5.5 in Fig. 6). As was the case for αRyR channels, a number of βRyR openings described by the shortest time constant (τ_{o1}) could not be resolved with our bilayer system. Therefore, the value given for this parameter is also an upper estimate.

The effects of channel modifiers

A number of agents have been found to alter the gating of the mammalian skeletal muscle RyR channel. These include Ca^{2+} ions (Smith et al., 1985, 1986), adenine nucleotides (Smith et al., 1985, 1986), caffeine (Rousseau et al., 1988; Rousseau and Meissner, 1989), and perchlorate anions (Ma et al., 1993), which generally increase, and Mg^{2+} and ruthenium red (Smith et al., 1986), which decrease channel activity. We therefore compared the ability of these agents to modify the behavior of the chicken skeletal muscle α- and βRyR ion channels. In the present studies, the effects of these agents were assessed on the *cis* (cytoplasmic) side of the bilayer.

Ca^{2+} and ATP

The effects of *cis* calcium in the absence and presence of 5 mM ATP on the activity of α- and βRyR channels are shown in Fig. 6, which presents single-channel records, and related to P_o in Fig. 7. As shown in these figures and in Fig. 4, in the absence of other modifiers, the α- and βRyRs are activated to different extents by Ca^{2+} ions. The P_o of αRyR channels in the low activity mode was activated to only modest levels (P_o < 0.3) by 30–100 μM Ca^{2+} and inhibited by greater levels of this cation (Fig. 7 *A*). In contrast, the same

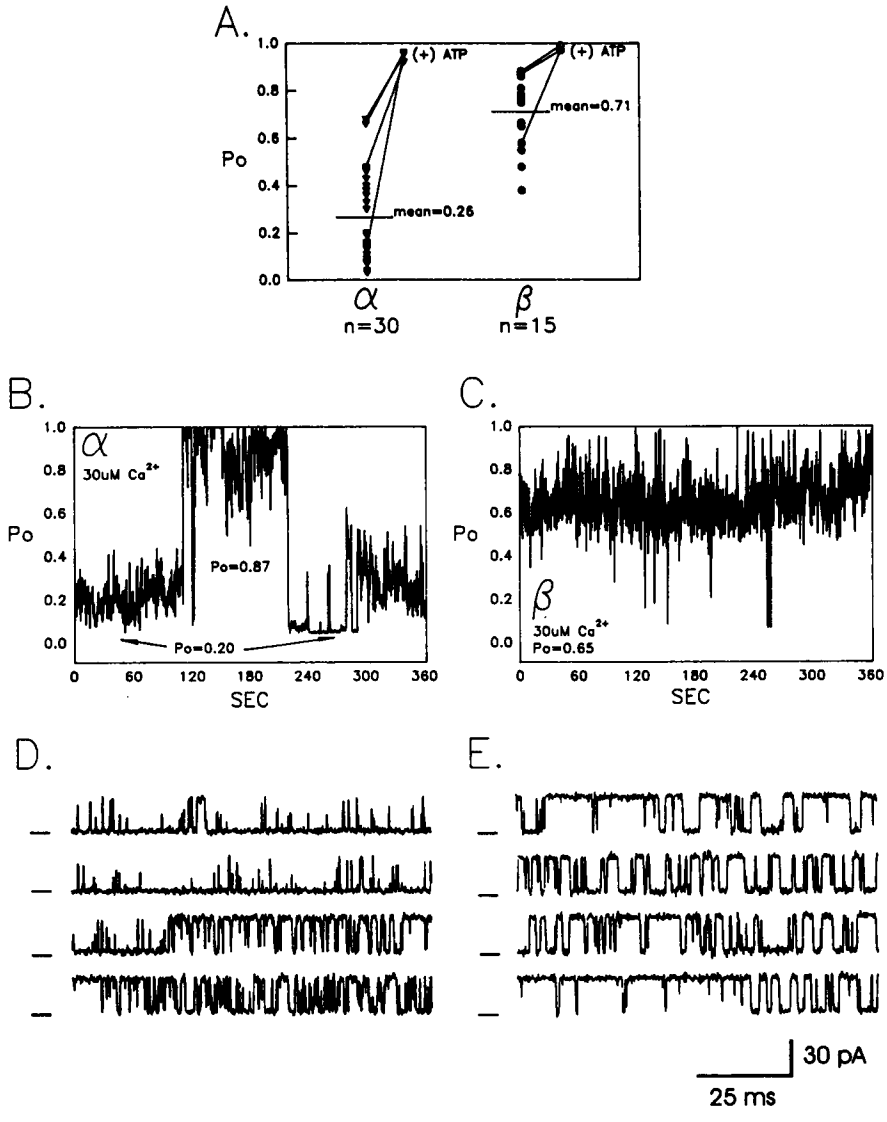

FIGURE 4 The αRyR is activated to a lesser extent by 30 μM (*cis*) Ca^{2+} than is the β isoform (*A*). The mean values shown are significantly different ($p < 0.05$). αRyR channels were distributed in two groups that exhibited low and intermediate P_o values. As shown in *B* and *D*, this was in part because of the ability of αRyR channels to switch between a low and high activity gating mode in a spontaneous and reversible manner. Note the transition from the low to the high activity mode in the third trace in *D*. The βRyR channel (*C* and *E*) also exhibited fluctuations in P_o, but these were much more rapid. Purified RyR channel activities were recorded in symmetrical 210 mM KCl and 30 μM *cis* Ca^{2+} at a voltage of −40 mV (*cis* negative). In the stationarity plots shown in *B* and *C*, P_o values were calculated every 256 ms. In *D* and *E*, zero current is indicated by the hash marks and openings are upward.

TABLE 1 Mean open channel lifetimes

Treatment/ channel type	P_o	τ_1 (ms)	Area (%)	τ_2 (ms)	Area (%)	τ_3 (ms)	Area (%)
30 μM Ca^{2+}							
0 α_L[0.05 ms]	0.12 ± 0.02 (11)	0.14 ± 0.01 (11)	91.8 ± 3.1	0.58 ± 0.06 (6)	15.0 ± 3.8	–	–
α_H [0.05 ms]	0.59 ± 0.07 (6)	0.17 ± 0.01 (6)	43.0 ± 7.3	0.51 ± 0.05 (6)	38.7 ± 3.6	1.27 ± 0.14 (6)	18.3 ± 5.5
β [0.05 ms]	0.71 ± 0.07 (7)	0.34 ± 0.03 (6)	14.8 ± 3.3	1.56 ± 0.34 (7)	63.1 ± 8.5	3.31 ± 0.97 (5)	33.8 ± 7.0
β [0.5 ms]	–	1.08 ± 0.27 (7)	54.4 ± 12.1	3.96 ± 0.76 (7)	45.6 ± 12.1	–	–
30 μM Ca^{2+} + ATP							
α_L [0.5 ms]	0.94 ± 0.02 (2)	1.27 ± 0.34 (2)	57.5 ± 2.5	5.23 ± 1.62 (2)	42.4 ± 2.5	–	–
α_H [0.5 ms]	0.94 ± 0.01 (3)	1.18 ± 0.09 (3)	17.3 ± 6.4	9.60 ± 3.14 (3)	82.7 ± 6.4	–	–
β [0.5 ms]	0.98 ± 0.01 (3)	0.52 ± 0.26 (3)	26.7 ± 16.5	42.05 ± 12.87 (3)	73.3 ± 16.5	–	–

Cumulative mean open channel time constants and values for the percent of the channels represented by a time constant obtained for the α_L, α_H, and βRyR channels activated by 30 μM *cis* Ca^{2+} ± 5 mM ATP. The bin size and the number of channels included in the analysis are shown in the square brackets and parentheses, respectively. Values given are means ± SEM. Purified RyR channel activities were recorded in symmetrical 210 mM KCl at a voltage of −40 mV (*cis* negative).

channels could be activated to much greater levels by 5 mM ATP + 30 μM Ca^{2+}. In the high activity mode, αRyR channels were activated more extensively by micromolar Ca^{2+}, reaching a P_o of 0.75 ± 0.01 ($N = 3$) in the presence of 30–200 μM Ca^{2+} (Fig. 7 *B*). Half-maximal activation was achieved at a Ca^{2+} concentration of 27.8 ± 3.3 μM ($N = 3$). In addition, α_H channels were inactivated by millimolar Ca^{2+} in the absence of ATP. Two α_H channels shown by the open

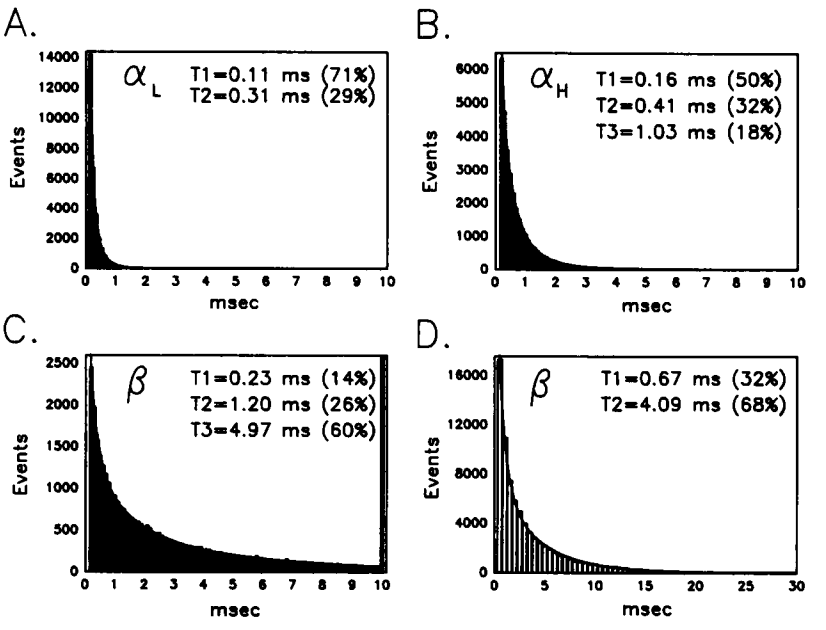

FIGURE 5 Dwell-time histograms constructed for resolved openings by αRyR channels in both the low (*A*) and high (*B*) activity gating modes and by the βRyR (*C* and *D*). A bin size of 0.05 ms was used in *A–C*. When this bin size was used for the βRyR channel a significant number of openings (~8000, *C*)) accumulated in the last bin and were excluded from the analysis. Therefore, this analysis was repeated using a 0.5 ms bin size to estimate the time constant for long openings more accurately (*D*). Purified RyR channel activities were recorded in symmetrical 210 mM KCl and 30 μM *cis* Ca^{2+} at a voltage of −40 mV (*cis* negative). Mean values for time constants derived for open and closed lifetimes of α- and βRyR channels and the percent of openings they represent are presented in Tables 1 and 2.

TABLE 2 Mean closed channel lifetimes

Treatment/ channel type	P_o	τ_1 (ms)	Area (%)	τ_2 (ms)	Area (%)	τ_3 (ms)	Area (%)
30 μM Ca^{2+}							
α_L[0.5 ms]	0.12 ± 0.02 (11)	0.86 ± 0.13 (11)	46.0 ± 6.3	4.25 ± 0.86 (11)	54.0 ± 6.3	–	–
α_H [0.5 ms]	0.59 ± 0.07 (6)	0.46 ± 0.06 (6)	83.7 ± 6.5	1.26 ± 0.17 (5)	19.6 ± 6.9	–	–
β [0.5 ms]	0.71 ± 0.07 (7)	0.53 ± 0.05 (7)	73.7 ± 9.5	1.51 ± 0.25 (6)	30.7 ± 9.5	–	–
30 μM Ca^{2+} + ATP							
α_L [0.5 ms]	0.94 ± 0.02 (2)	0.16 ± 0.02 (2)	100 ± 0	–	–	–	–
α_H [0.5 ms]	0.94 ± 0.02 (3)	0.18 ± 0.08 (3)	94.3 ± 5.7	0.89 ± 0.00 (1)	17.0 ± 0.0	–	–
β [0.5 ms]	0.98 ± 0.01 (3)	0.25 ± 0.03 (3)	94.7 ± 1.8	0.85 ± 0.04 (3)	5.3 ± 3.1	–	–

Cumulative mean closed channel time constants and values for the percent of the channels represented by a time constant obtained for the α_L, α_H, and βRyR channels activated by 30 μM *cis* Ca^{2+} ± 5 mM ATP. The bin size and the number of channels included in the analysis are shown in the square brackets and parentheses, respectively. Values given are means ± SEM. Purified RyR channel activities were recorded in symmetrical 210 mM KCl at a voltage of −40 mV (*cis* negative).

and filled inverted triangles in Fig. 7 *B* showed a decline in P_o in the presence of micromolar Ca^{2+}. This decline in the activity of these two α_H channels was probably caused by a switch from the high to the low (Ca^{2+}-insensitive) activity mode during the course of the experiment rather than by an inhibition of channel activity by 30–300 μM Ca^{2+}. The occurrence of this switch is supported by the observations that channel activity was not increased by returning to lower Ca^{2+} concentrations that previously had activated the channels. In addition, both channels were activated by the subsequent addition of 5 mM ATP in a manner similar to that observed for the α_L channels shown in Fig. 7 *A*.

In the presence of 5 mM ATP, αRyR channels were much more active over a wide range of Ca^{2+} levels than before addition of the nucleotide (Fig. 7 *D*). This presumably represents the behavior of both α_L and α_H channels, which cannot be distinguished under these conditions. The extent of channel activation by 30 μM Ca^{2+} before the addition of ATP is indicated by the individual symbols in Fig. 7 *D*. In the presence of ATP, maximal activation to a P_o of 0.95 ± 0.01 (N = 4) was observed in the presence of 30–200 μM Ca^{2+}. Moreover, αRyR channels were more active at lower Ca^{2+} concentrations in the presence than in the absence of nucleotide, with P_o values >0.5 being observed in submicromolar Ca^{2+} in two cases. The other channels shown were half-maximally activated by 3.6 and 4.4 μM Ca^{2+}. Increasing *cis* Ca^{2+} to millimolar concentrations resulted in channel inactivation. Half-maximal inhibition was observed at 2.12 ± 0.62 mM Ca^{2+} (N = 3). As shown in Fig. 7 *D*, αRyR channels varied in their sensitivity to both the activating and inactivating effects of Ca^{2+} ions. The basis of this variability and the possible involvement of unappreciated switching between the two gating modes is currently being assessed.

In the absence of ATP, βRyR channels were sensitive to both activation and inhibition by Ca^{2+} ions (Fig. 7 *C*). Half-maximal and maximal activation of βRyR channels were observed in 14.0 ± 1.6 and 20–200 μM Ca^{2+}, respectively (N = 4). βRyR channels were activated to a greater relative extent by Ca^{2+} than by Ca^{2+} + 5 mM ATP with maximal activation increasing P_o from 0.75 ± 0.05 (N = 4) in the absence of ATP to ~1.0 (N = 3) in the presence of nucleotide + Ca^{2+} >20 μM. Moreover, in the presence of ATP the

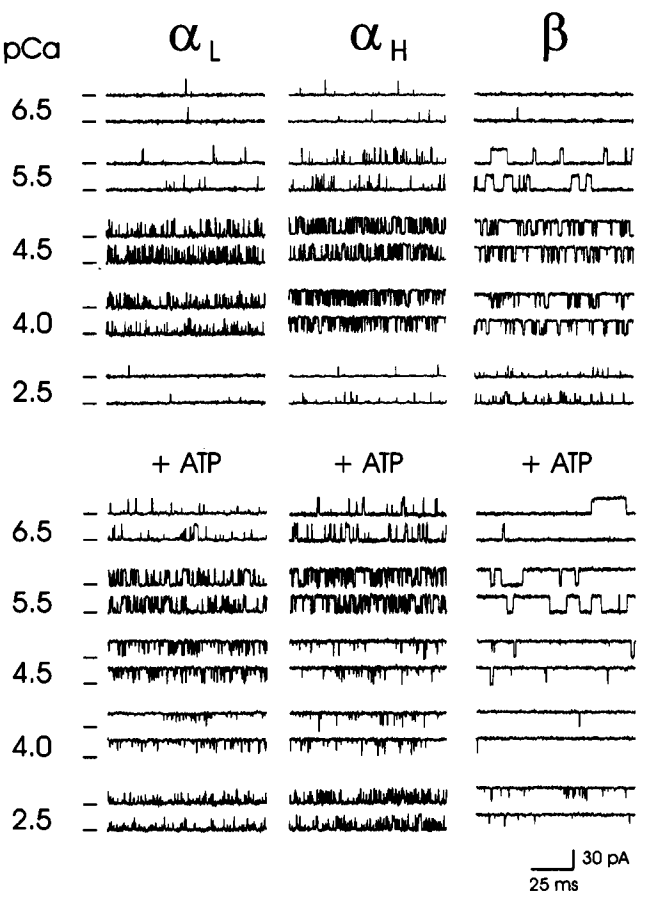

FIGURE 6 Representative single-channel current traces recorded in the presence of different *cis* (cytoplasmic) Ca^{2+} levels in the absence and presence of 5 mM ATP from αRyR channels in both low (α_L) and high (α_H) gating modes and from a βRyR channel. Purified RyR channel activity was recorded in symmetrical 210 mM KCl at a voltage of −40 mV (*cis* negative). Note the differences in channel lifetimes between the α- and βRyR channels and in the responses by all three channel behaviors to the activating and inactivating effects of micromolar and millimolar *cis* Ca^{2+}. These results are summarized in Fig. 7. Zero current is indicated by the hash marks and openings are upward.

activating effect of micromolar Ca^{2+} was enhanced, with half-maximal activation occurring at 1.8 ± 0.3 μM Ca^{2+} ($N = 3$, Fig. 7 *E*). The inhibition of βRyR channel activity by millimolar Ca^{2+} (half-maximal inhibition at 1.36 ± 0.43 mM Ca^{2+}, $N = 3$) observed in the absence of ATP was no longer evident in the presence of nucleotide. The extent of activation of βRyR channels in the presence of Ca^{2+} ± ATP was less variable than that observed for αRyR channels. Thus, βRyR channels were activated half-maximally by Ca^{2+} concentrations that were ~2-fold lower than those required for a similar activation of α_H channels, both in the absence and presence of ATP. In the presence of ATP, the concentration of Ca^{2+} required for half-maximal activation was decreased by a factor of 7 for both α_H and βRyR channels. The effects of both Ca^{2+} and ATP on the activity of α- and βRyR channels were fully reversible after perfusion of the *cis* chamber.

Although activation and inactivation of α (α_H) and βRyR channels by micromolar and millimolar Ca^{2+}, respectively, resulted in comparable changes in P_o, different relative changes occurred in the mean open and closed lifetimes of each channel type. This can be appreciated from comparisons of the gating behavior of the channels at three different levels of activation: suboptimal activating Ca^{2+} (10 μM), maximally activating Ca^{2+} (30 μM), and inhibiting Ca^{2+} (1–3 mM). To permit more direct comparisons of the gating exhibited by both channels under these different conditions, dwell-time histograms were normalized by conversion to probability density functions (Colquhoun and Sigworth, 1983) to adjust for differences in the total number of events in each record (Fig. 8 *A–D*). The relationships observed between the mean open and closed channel lifetimes for both the α_H and β channels in the three different states of activation are shown in Fig. 8 *E* and Table 3.

As shown, an increase in *cis* Ca^{2+} from 10 to 30 μM increased the P_o of an α_H channel from 0.13 to 0.87 and involved an increase and decrease in mean open and closed times, respectively, that were of similar magnitude. For comparison, a βRyR channel exhibiting a comparable increase in P_o (0.16 to 0.86) with a change in Ca^{2+} from 10 to 100 μM, but in this case there was a larger decrease in mean closed time than increase in mean open time. Similar differences in the relative changes in mean channel lifetimes were observed when *cis* Ca^{2+} was increased to levels (3 mM) that inhibited both channel types. For example, the change in α_H channel P_o (0.87 to 0.11) again involved similar relative changes in mean open and closed times. A comparable change in the β channel P_o (0.86 to 0.14) resulted from a larger decrease in mean open time than increase in mean closed time.

The net result of these changes was that α_H channels exhibited comparable P_o values and gating behaviors at suboptimal activating (10 μM) and inhibiting (1 mM) Ca^{2+} (Fig. 8, *A*, *C*, and *E*; also compare the current traces recorded in pCas of 5.5 vs. 2.5 in Fig. 6). In contrast, although βRyR channels also exhibited similar P_o values at low micromolar and millimolar Ca^{2+}, quite different channel gating behaviors were observed under these different activating conditions. The shift to predominantly short openings and closings in inhibiting (3 mM) Ca^{2+} caused βRyR channels to resemble αRyR channels in their gating, much more than that of βRyR channels in suboptimal activating Ca^{2+} levels (Fig. 8, *B*, *D*, and *E*; also again compare current traces recorded in pCas of 5.5 vs. 2.5 in Fig. 6).

Unlike the case for Ca^{2+} alone, activation of α_HRyR channels by 5 mM ATP + 30 μM Ca^{2+} involved dramatic changes in both channel open and closed times, but the increase in open times was larger than the decrease in closed times (16.3- vs. 2.9-fold) (Table 3). Similarly, for βRyR channels activation by ATP resulted in a greater increase in mean open times than decrease in mean closed times (13.0- vs. 3.0-fold), which is the opposite of the relative changes produced in open and closed channel lifetimes during activation by Ca^{2+} (Table 3). The magnitudes of the changes in channel lifetimes were such that α_HRyR channels activated to comparable P_o values by Ca^{2+} or by Ca^{2+} + ATP had

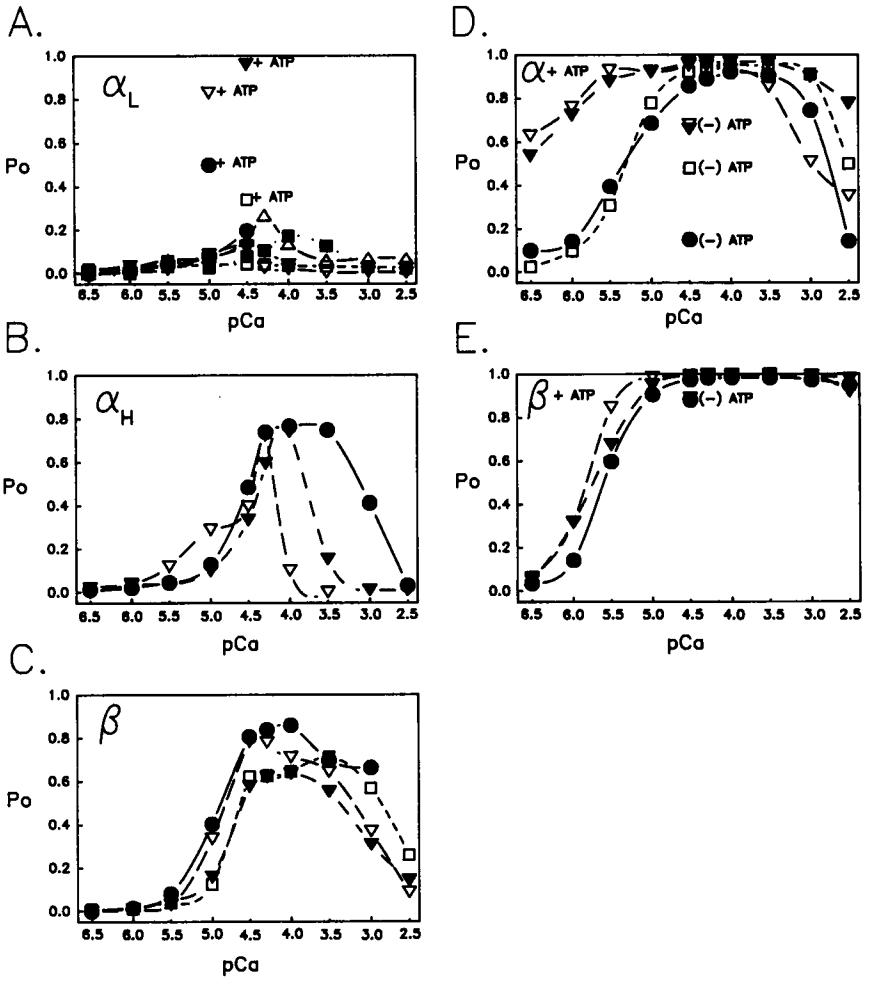

FIGURE 7 The responses of purified α channels in both the low (α_L) (*A* and *D*) and high (α_H) (*B* and *D*) activity gating modes, and βRyR channels (*C* and *E*) to activation and inactivation by Ca^{2+} in the absence (*A–C*) and presence (*D* and *E*) of 5 mM ATP. The individual symbols shown in *A* and *D* indicate the P_o values obtained for the different channels in either the presence (*A*) or absence (*D*) of added ATP. The individual symbols labeled "+ATP" in *A* indicate the P_o of the same channel indicated by the connected symbols after the addition of 5 mM ATP. The individual symbols labeled "(−) ATP" in *D* indicate the P_o of the same channel indicated by the connected symbols before the addition of 5 mM ATP. In *B*, two channels (▽, ▼) switched from the high to the low activity mode at the peak of the Ca^{2+} response curve. Both of these channels could still be activated by ATP. Purified RyR channel activity was recorded in symmetrical 210 mM KCl at a voltage of −40 mV (*cis* negative).

similar gating behaviors. In contrast, βRyR channels activated by Ca^{2+} and by Ca^{2+} + ATP had quite different gating kinetics. This can be appreciated by comparing the current traces for the channels shown in Fig. 6 recorded in a pCa of 4.5 in the absence with those recorded in a pCa of 5.5 + ATP (conditions that produce comparable P_o values, e.g., Fig. 7). Effects similar to those noted above for ATP were also obtained with AMP.

Caffeine

The activating effects of caffeine were tested in the presence of 10 μM Ca^{2+}, which is suboptimal for channel activation. Caffeine at concentrations of 1–10 mM produced similar increases in the activities of both α- and βRyR channels (n = 3). For example, as shown in Fig. 9, 1 mM caffeine increased the P_o observed for α- and βRyR channels from O.19 to 0.35 and 0.20 to 0.46, respectively.

Ruthenium red and Mg^{2+}

These agents decrease the P_o of mammalian RyR channels (Smith et al., 1986); therefore, the chicken skeletal muscle RyR channels were exposed to ATP + 10 μM Ca^{2+} to permit the effects of these agents to be tested at comparable levels of channel activation. Each of these agents diminished the P_o of the α- and βRyR channels. Ruthenium red (1 μM, n = 2–3) essentially abolished all channel activity (Fig. 9). When Ca^{2+} was maintained at a constant level, the addition of 0.5 mM Mg^{2+} exerted similar and marked inhibitory affects on both α- and βRyR channels (n = 3). For example, as shown in Fig. 9, this level of Mg^{2+} reduced the P_o of an αRyR channel from 0.69 to 0.02 and that of a representative βRyR channel from 0.84 to 0.14.

Ryanodine

The hallmark for RyR channels is modification by micromolar levels of the plant alkaloid ryanodine to a conformation exhibiting a long-lived subconductance state (Rousseau et al., 1987; Imagawa et al., 1987). Consistent with our previous identification of both proteins as RyR isoforms based on [^{3}H]ryanodine binding (Airey et al., 1990), both the α- and βRyR channels (n = 5) were modified to subconductance states with similar amplitudes (59% of full opening) by 0.1 μM ryanodine (Fig. 10).

Voltage

The activity of both the α- and βRyR channels was sensitive to the voltage applied across the bilayer. Making the *cis* (cytoplasmic) side of the bilayer negative relative to the *trans*

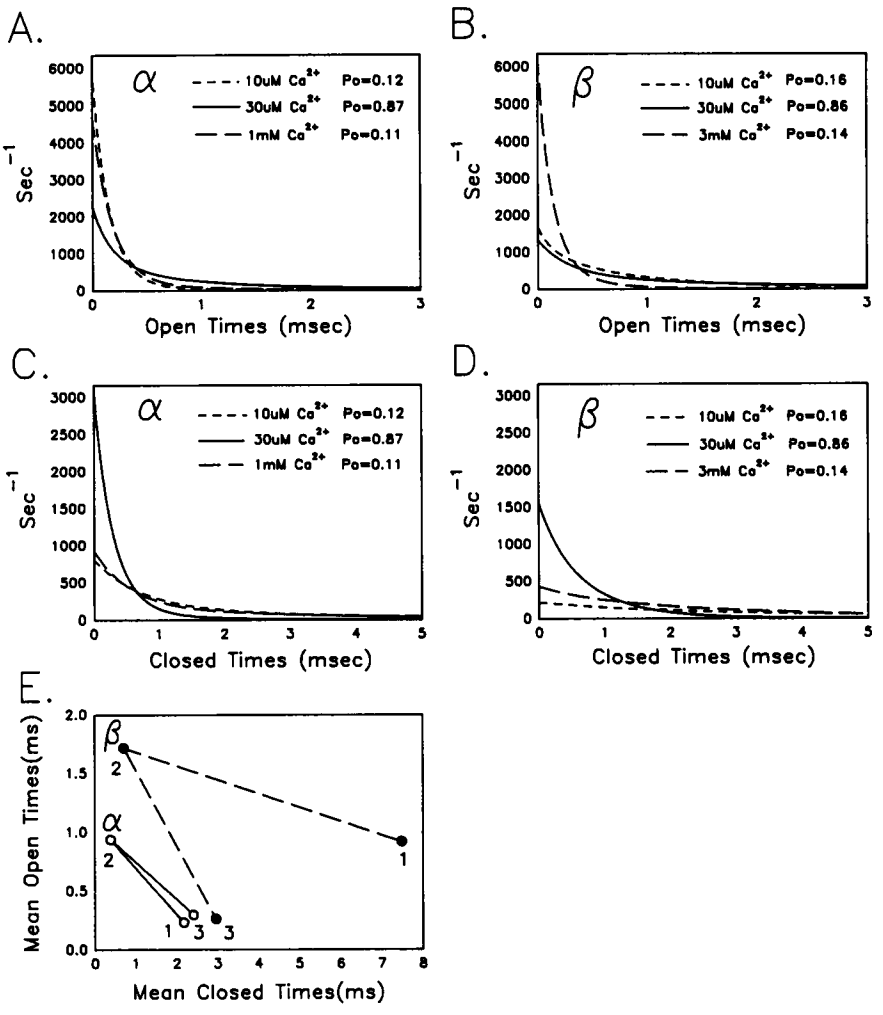

FIGURE 8 (*A–D*) Probability density functions derived for the open and closed event durations exhibited by an α_H and a βRyR channel in the presence of suboptimal (10 μM), maximally activating (30 μM), and inhibiting (1–3 mM) *cis* Ca^{2+} concentrations. (*E*) The relationships between the mean open and closed times obtained for both channels (α_H, ○; β, ●) under the different activating conditions (1 = suboptimal; 2 = maximally activating; 3 = inhibiting Ca^{2+}). Channel currents were recorded in symmetrical 210 mM KCl at −40 mV (*cis* negative).

TABLE 3 Alteration of α_H and βRyR mean channel lifetimes by Ca^{2+} and ATP

	Mean open lifetimes (ms)	
	α_HRyR	βRyR
Ca^{2+} (10 μM)	0.17 [0.12]	0.92 [0.16]
Ca^{2+} (30 μM)	0.94 [0.87]	1.72 [0.86]
Ca^{2+} (1–3 mM)	0.30 [0.11]	0.21 [0.14]
Ca^{2+} (30 μM)	0.50 [0.59]	2.39 [0.71]
Ca^{2+} (30 μM) + ATP (5 mM)	8.14 [0.94]	30.96 [0.98]
	Mean closed lifetimes (ms)	
Ca^{2+} (10 μM)	1.03	7.48
Ca^{2+} (30 μM)	0.38	0.70
Ca^{2+} (1–3 mM)	2.40	2.95
Ca^{2+} (30 μM)	0.63	0.85
Ca^{2+} (30 μM) + ATP (5 mM)	0.22	0.28

Mean open and closed lifetimes for the α and βRyR channel currents recorded in suboptimal activating Ca^{2+} (10 μM), maximally activating Ca^{2+} (30–100 μM) and inhibiting Ca^{2+} (3 mM) and in maximally activating Ca^{2+} in the absence and presence of 5 mM ATP. The P_o values observed under each condition are shown in the square brackets. The upper three values in each column are from a single channel, whereas the lower two values represent mean values taken from Tables 1 and 2.

(luminal) side resulted in continuous channel activity. In contrast, making the *cis* (cytoplasmic) side of the bilayer positive led to the appearance of a long-lived closed state (Fig. 11). After such closings, a change back to a negative polarity (noted by the asterisk in Fig. 11) was generally required to reinitiate channel openings. Although these effects have not yet been studied in detail, the inhibitory effect of positive voltages was seen within seconds of switching to voltages ≥+40 mV. This effect depended in an inverse manner on both the magnitude of the imposed voltage and time (e.g., the larger the applied voltage, the shorter the time required for channel inactivation).

Perchlorate

The results of recent studies suggest that perchlorate anions affect the SR Ca^{2+} release activation process in skeletal muscle cells involving interactions between the dihydropyridine receptors and RyR (for references, see Gallant et al., 1993; Gonzalez and Rios, 1993; Ma et al., 1993;). Consistent with this possibility, E-C coupling in mammalian cardiac and crayfish skeletal muscles, which utilizes a Ca^{2+}-induced Ca^{2+} release mechanism to activate SR Ca^{2+} release, was not affected by perchlorate (Ma et al., 1993; Gyorke and Palade, 1992). Moreover, perchlorate anions appear to activate the RyR channel directly through actions at an inorganic phosphate binding site (Fruen et al., 1994a, b).

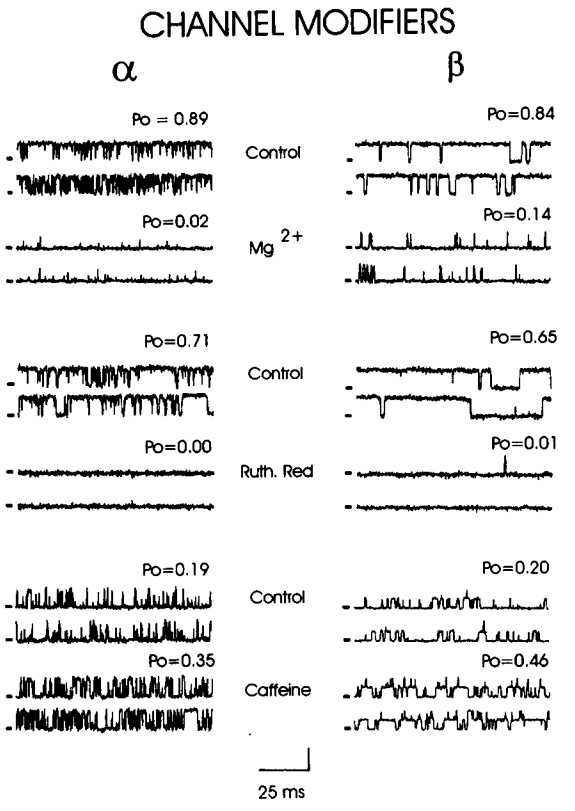

FIGURE 9 The effects of the RyR channel inhibitors, Mg^{2+} (0.5 mM, *top panels*) and ruthenium red (1 μM, *middle panels*), and the channel activator, caffeine (1 mM, *bottom panels*), on α (*left panels*) and βRyR (*right panels*) channel activity. The P_o values obtained for each condition are shown above the corresponding pair of current traces. Purified RyR channel activities were recorded in symmetrical 210 mM KCl at a voltage of -40 mV (*cis* negative). Channels were activated by 10 μM Ca^{2+} + 5 mM ATP in the Mg^{2+} and ruthenium red studies and by 10 μM Ca^{2+} in the caffeine experiments. Zero current is indicated by the hash marks and openings are upward. The vertical calibration bar represents 30 pA for all traces except those showing the responses of βRyR channels to caffeine. In the latter case, the calibration bar indicates 50 pA, as a lower gain was used to plot the currents from two β channels present in this bilayer.

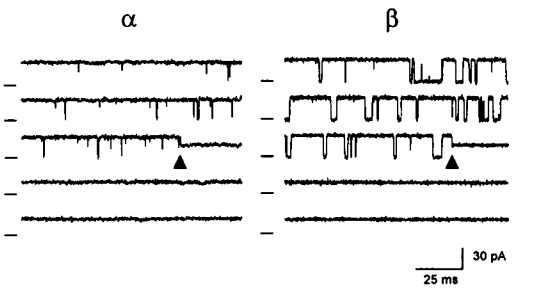

FIGURE 10 Modification of purified α (*left*) and β (*right*) RyR channels by 0.1 μM ryanodine to a long-lived subconductance state. The modification indicated by the arrowheads occurs in the third trace in each panel. Currents were recorded in symmetrical 210 mM KCl at a voltage of -40 mV (*cis* negative). 10 μM Ca^{2+} and 5 mM ATP were added to the *cis* (cytoplasmic) chamber to activate the channels. Ryanodine (0.1 μM) was subsequently added to the *cis* chamber. Zero current is indicated by the hash marks and openings are upward. For both α and β channels, the amplitude of the substate current was 59% of that observed for the full open state recorded before the addition of ryanodine.

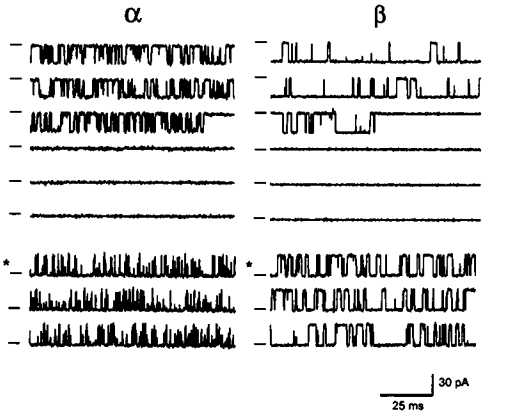

FIGURE 11 Inactivation of purified α (*left*) and βRyR (*right*) channels by the imposition of positive voltages (*cis* or cytoplasmic side positive). The voltage was changed from -40 to $+40$ mV just before the start of the first current trace. Shortly before the seventh current trace, indicated by the asterisk, the voltage was changed back to -40 mV to demonstrate reactivation of the channel. The records shown are consecutive. The current traces shown were recorded in symmetrical 210 mM KCl at a voltage of $+40$ mV (*cis* positive). 3 μM Ca^{2+} and 5 mM ATP were present in the *cis* chamber. Zero current is indicated by the hash marks.

We used protocols developed by Ma et al. (1993) to assess whether perchlorate affected either of the chicken skeletal muscle RyRs. In these studies, the probability of channel opening was decreased before exposure to perchlorate by adding either 5 mM $MgCl_2$ to block the channel (n = 3) or EGTA to decrease the concentration of activating Ca^{2+} in the *cis* chamber to submicromolar levels (n = 6–8). As shown in the left panels of Fig. 12, perchlorate anions (20 mM) increased the activity of the αRyR channel in a manner similar to that observed for the rabbit skeletal muscle RyR (Ma et al., 1993). In contrast, perchlorate anions (20–40 mM) did not produce similar increases in the activity of βRyR channels (Fig. 12, *right* panels). Comparable results were obtained using EGTA to decrease channel activity (data not shown).

Microsomal membranes: ryanodine-sensitive channel activities

The purification of integral membrane proteins involves the possibility that the functional properties of the protein may be altered. This can be caused by either the procedures utilized to extract the protein from membranes or a failure to establish conditions that reproduce those in native membranes when assaying protein activity. The chicken skeletal muscle α- and βRyRs differ in their biophysical properties. For example, the α- and βRyRs differ in the ease with which they incorporate into bilayers. It is more difficult to fuse the αRyR, with relatively longer periods of stirring being required, whereas βRyRs fuse more readily, and frequently multiple βRyR channels are incorporated. In addition, [^{3}H]-ryanodine binding by each isoform is altered differently by changes in the concentrations of CHAPS and PC (data not shown). Such behavior suggested that the ion channel properties of these proteins could be influenced differentially by

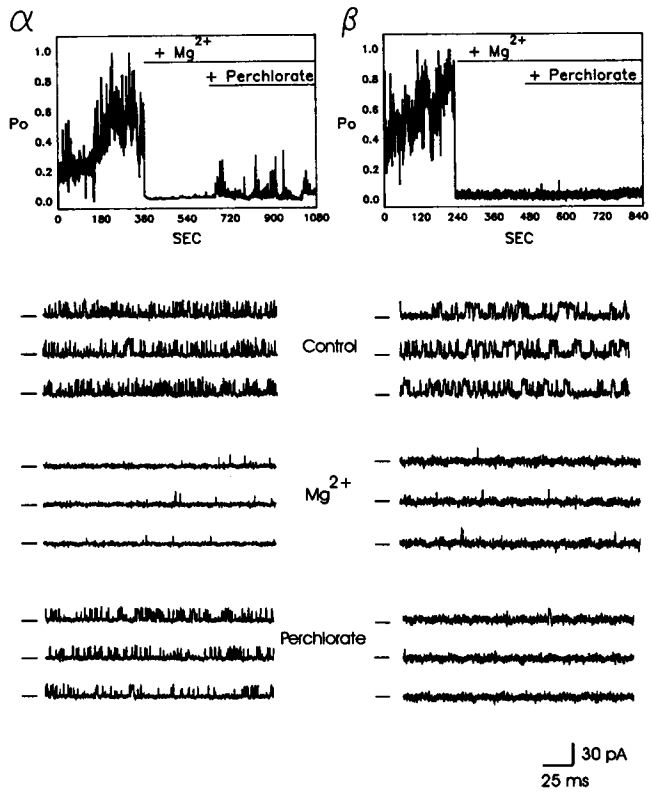

FIGURE 12 Perchlorate activates purified α, but not β, RyR channels. Stationarity plots (P_o values calculated every 256 ms) are shown in the top left panel for α and top right panel βRyR channels. Corresponding current traces recorded in symmetrical 210 mM NaCl at a voltage of -40 mV (*cis* negative) are shown in the left (α) and right (β) panels. 30 μM Ca^{2+} was added to both the *cis* and *trans* chambers. After 4–6 min of recording under control conditions, 5 mM Mg^{2+} was added to both *cis* and *trans* chambers to inhibit channel activity. After an additional 3–5 min of recording, 20 mM Na perchlorate was added to both the *cis* and *trans* chambers. Note that perchlorate activates the α, but not the β, RyR channel. Zero current is indicated by the hash marks and openings are upward.

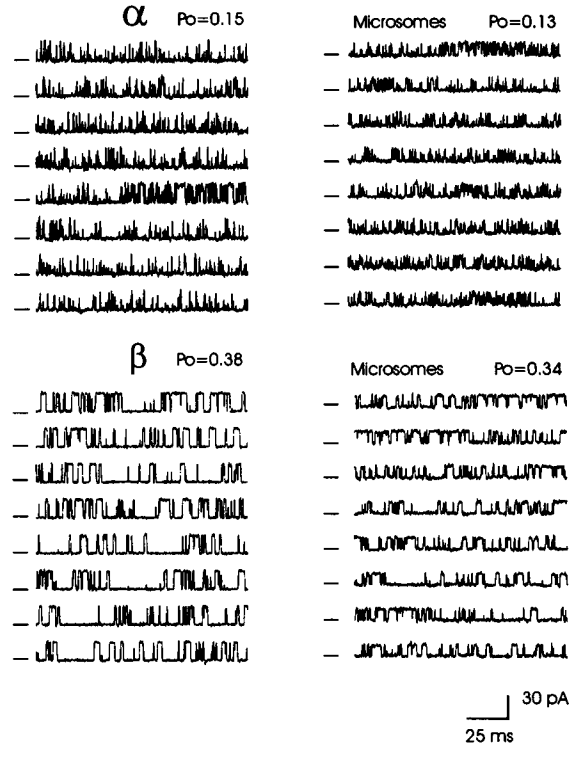

FIGURE 13 RyR channels having properties similar to those observed for the purified α (*top left*) and β (*bottom left*) RyR channels are observed after fusion of native SR membranes with bilayers (*right panels*). Purified RyR channel activities were recorded in symmetrical 210 mM KCl and 30 μM *cis* Ca^{2+} at a voltage of -40 mV (*cis* negative). RyR channels derived from native SR membranes were recorded in symmetrical 210 mM CsCl. Note the amplitude of the currents recorded in CsCl is less than that of ones recorded in KCl. The respective P_o values for each preparation are given above each set of current traces. Zero current is indicated by the hash marks and openings are upward.

the protein purification and/or assay systems used. To investigate this possibility, we assessed whether ryanodine-sensitive channels with properties similar to those found for purified α- and βRyRs were observed after fusion of native SR membranes with the bilayer.

RyR channels with conductance and gating characteristics similar to those of the purified receptor proteins were obtained after incorporation of SR membranes (Fig. 13). Channels like those observed with purified αRyRs, exhibiting very short, spike-like openings were found. These channels also mimicked αRyR channels in their relative sensitivities to activation by Ca^{2+} in the presence and absence of ATP and the observation of both the low and high activity gating modes. A second channel type that had longer openings and a greater sensitivity to activation by Ca^{2+} than by ATP, similar to the purified βRyR, was also observed (Fig. 13). The difference in the current amplitudes obtained for purified and SR membrane-derived RyR channels is due to the use of K^+ and Cs^+, respectively, as the charge carrier. The Cs^+ conductances of purified and membrane-derived channels were identical.

DISCUSSION

The results of the present studies lead to two general conclusions. First, both the α- and the βRyR isoforms in chicken skeletal muscle fibers embody ryanodine-sensitive Ca^{2+} channels having similar conductance characteristics. Second, the chicken skeletal muscle receptor isoforms differ in their gating behaviors, in the extent and manner in which they respond to activation and inactivation by Ca^{2+} and activation by ATP and in a number of physical properties.

Both of the chicken skeletal muscle RyR isoforms form high conductance Ca^{2+} channels and in this regard, they are similar to the two RyR isoforms co-expressed in frog skeletal muscles (Murayama and Ogawa, 1992; Bull and Marengo, 1993). The conductances and relative permeabilities of mono- and divalent cations are similar for the chicken α- and βRyR isoforms. The conductance properties observed for these proteins in the present studies are generally similar to those reported for the mammalian RyR isoforms (Williams, 1992), indicating that the functional attributes of the conduction pore in this protein have been conserved between these species. The conductance of both the α- and βRyR channels was greater for K^+ than for Cs^+. In this regard, the chicken skeletal muscle receptors resemble the RyR ex-

pressed in sheep heart, which has the same conductance order for these cations (Lindsay et al., 1991), but differ from the rabbit skeletal muscle RyR, which has a conductance order of $Cs^+ > K^+$ (Smith et al., 1988). A $P_{Ca^{2+}}/P_{K^+}$ ratio of 7.4 was observed for both the α- and βRyR channels, which is identical to the value observed for the sheep cardiac RyR (Lindsay and Williams, 1991) and comparable to that (6.6) reported for the rabbit skeletal muscle receptor (Smith et al., 1988).

Although the α- and βRyR channels have similar conductance characteristics, they have marked differences in their gating properties and their relative responses to Ca^{2+} and ATP.

αRyR

αRyR channels are characterized by having short, spike-like openings at all levels of activation. The P_o values observed for different αRyR channels in 30 μM (*cis* or cytoplasmic) Ca^{2+} varied over a 14-fold range. This extensive variability is caused, at least partially, by the ability of these channels to assume two gating modes. αRyR channels can reside in either mode in a relatively stable fashion, e.g., for minutes at a time, and they can switch between gating activities in a reversible manner. Channels in the two gating modes differ in the extent that they can be activated by Ca^{2+} and ATP. For example, in the low activity mode, αRyR channels have low P_o values and are minimally responsive to the activating effects of Ca^{2+} in the absence of ATP, whereas channels in the high activity mode have greater P_o values in response to activation by Ca^{2+}. The switch from the low to the high activity mode involves the appearance of a new open state characterized by a longer time constant (Table 1). This suggests that the switch results from the opening of a new pathway to a longer-lived open state and a consequent destabilization of a closed state or states.

Ion channel activity is regulated by stabilization of the channel protein in conformations having specific gating properties. It is likely that channel proteins can spontaneously assume these same conformations in the absence of channel modifiers, albeit less stably. Thus, the ability of the αRyR channel to exhibit two quite different gating modes suggests that regulation of this channel has dramatic effects on its activity as a Ca^{2+} release channel in situ, influencing both activation and inactivation. Meissner et al. (1989) have shown that limited proteolysis causes activation of the mammalian skeletal muscle RyR channel. The observation that αRyR channels can switch between the two gating modes in a reversible manner demonstrates that although an irreversible change, such as proteolysis, or other forms of protein degradation, e.g., unfolding, could stabilize one of the conformations, it is not required for switching. Reversible processes, such as protein phosphorylation (Witcher et al., 1991; Takasago et al., 1991; Wang and Best, 1992; Yoshida et al., 1992; Herrmann-Frank and Varsanyi, 1993) or the binding of a modulating ligand, could also stabilize the protein in one of the gating modes. An example of the latter could be the FK506 binding protein, a peptidyl-prolyl *cis*-trans isomerase, which has been found recently to influence the activity of the mammalian skeletal muscle RyR isoform (Jayaraman et al., 1992; Timerman et al., 1993). We are currently investigating the influences of these as well as of other types of channel protein modifications. The alterations in the activity of L- and N-type Ca^{2+} channels produced by dihydropyridines and norepinephrine, respectively, have been shown to result from stabilization of conformations of these proteins having different gating modes (Hess et al., 1984; Nowycky et al., 1985; Delcour and Tsien 1993).

The variability in the αRyR channel responses to both the activating and inactivating effects of Ca^{2+} observed in the presence of ATP (Fig. 7 *D*) suggest that more than one type of modification is involved. It is possible that the variable responses to the inactivating effects of high concentrations of Ca^{2+} were caused in part by a switch from the high to low gating mode during the course of the experiment. Because channels in both modes have similar P_o values in the presence of micromolar Ca^{2+} + ATP, a switch between the modes would not have been detectable under these conditions. It will be important to establish the basis of this variability in activation and inactivation states to understand the in situ role of this ion channel in skeletal muscle E-C coupling.

βRyR

The most numerous βRyR channel openings are significantly longer than those observed for αRyR channels, and the identity of these channels can be established on this basis in low levels of activating Ca^{2+} (e.g., compare the current traces recorded in a pCa of 5.5 shown in Fig. 6). The P_o values recorded for βRyR channels in 30 μM *cis* Ca^{2+} were also variable, but over a narrower range (2.25-fold) than was observed for αRyR channels. In comparison with those of αRyR channels, the responses of the βRyR channels to Ca^{2+} + ATP were more reproducible from experiment to experiment. Single βRyR channels exhibited spontaneous variations in activity. The transitions between these different activity levels were very rapid and similar to those reported for a number of channel types. Millimolar concentrations of Ca^{2+} inhibited βRyR channel activity, but only in the absence of ATP.

α vs. βRyR

The different nature of the α- and βRyR channels is indicated by the activation of β channels by lower Ca^{2+} concentrations than those required to activate α channels, and by the manner in which these channels responded to activation and inhibition by Ca^{2+} and to activation by ATP. Activation of αRyR channels by Ca^{2+} involved relatively similar changes in mean open and closed times. Inhibition of αRyR channel activity by high Ca^{2+} levels resulted from the reversal of these changes. The relative magnitudes of the changes in both open and closed times are such that αRyR channels maintain their short, spike-like opening pattern at all levels of activation and

in both Ca^{2+} and Ca^{2+} and ATP (cf. Fig. 6). The αRyR channel had more very short (unresolved) openings in the presence of suboptimal Ca^{2+} than in inhibiting Ca^{2+}. In contrast, activation of βRyR channels by Ca^{2+} involved a greater decrease in mean closed time than increase in mean open time. Inhibition of βRyR channels by millimolar Ca^{2+} involved greater changes in mean open time than in mean closed time. As can be appreciated from the current traces shown in Fig. 6, the relative magnitudes of these changes cause βRyR channels to have quite different gating behaviors in the presence of different *cis* Ca^{2+} concentrations. For example, in millimolar Ca^{2+}, βRyRs resemble αRyR channels.

In contrast to the differences in the changes produced in the gating of the α and β channels by Ca^{2+}, the behavior of both channel types was altered in a similar manner during activation by ATP (Table 3). This involved marked increases in open channel lifetimes accompanied by more modest decreases in closed times. Thus, although similar P_o values are attained, the gating behaviors of the α- and βRyR channels differ depending on whether they are activated by Ca^{2+} or ATP. In the case of βRyR channels, Ca^{2+} appears to destabilize a closed state, whereas ATP stabilizes an open state. Whether such differences in channel behavior at the single-channel level are important to the contributions made to the SR Ca^{2+} release transient by each channel type remains to be determined. The importance of the effects of adenine nucleotides on the activity of both the α- and βRyR channels in situ is not understood. If either the levels of nucleotide in the vicinity of the RyR channels or the influences exerted by the nucleotides on the channels vary under physiological conditions, the activity of both RyR channels could be altered dramatically. The differences between α- and βRyR channel open durations were even more marked in the absence of ATP, where α channels exhibited a larger number of openings that were too brief to be resolved with the bilayer system. Although the physiological significance of such very short openings remains to be determined, it may be speculated that they are more efficient at providing Ca^{2+} for activation of adjacent channels than for increasing Ca^{2+} in the vicinity of the myofibrils. Clarification of the importance of the regulatory influences of adenine nucleotides may require the expression of mutant RyRs in which nucleotide binding has been abolished in an otherwise normal muscle cell background. As recently shown by Sanchez and Vergara (1994), analysis of the effects of ATP released from caged ATP on SR Ca^{2+} release may also provide insights into this issue.

Although two RyR isoforms are also co-expressed in skeletal muscles in frogs and fish, systematic investigations of the ion channel properties of the receptor isoforms in these species have not been reported. There have been several reports concerning the ion channel properties of the RyRs expressed in frog skeletal muscles (Suarez-Isla et al., 1991; Murayama and Ogawa, 1992; Bull and Marengo, 1993). Murayama and Ogawa (1992) have shown that each of the frog RyR isoforms embodies an ion channel that is activated by both Ca^{2+} and ATP and inhibited by ruthenium red. Bull and Marengo (1993) observed channels exhibiting different sensitivities to activation by Ca^{2+} after fusion of frog skeletal muscle SR membranes with bilayers. One channel type was activated half-maximally by ~10 μM Ca^{2+}, maximally activated (P_o ~0.6) by ~30 μM Ca^{2+}, and inhibited by Ca^{2+} concentrations ≥100 μM. The second channel type was activated to half-maximal levels by ~1 μM Ca^{2+}, reached a maximal P_o of ~1.0 in ~30 μM Ca^{2+}, and was not inhibited by Ca^{2+} concentrations up to 1 mM. The difference in the Ca^{2+} concentrations required for activation of these channels is similar to that observed for the chicken α- and βRyR receptors in the present studies. Given the variability we have observed in the activation of the chicken α- and βRyR isoform channels, the ability of ATP to change the sensitivity of both of the chicken channel types to the activating and inactivating effects of Ca^{2+}, and the fact that the results of Bull and Marengo were obtained with intact SR membranes containing both RyR isoforms, it is difficult to compare their data with those we have obtained with purified RyRs in a more specific manner.

The results of the present studies offer some suggestions concerning the possible roles of each of the chicken skeletal muscle RyR isoforms in E-C coupling in situ. As noted in the Introduction, two mechanisms have been proposed to activate the release of SR Ca^{2+} in skeletal muscles. The first involves interactions between dihydropyridine receptor and RyRs, whereas a Ca^{2+}-induced Ca^{2+} release mechanism underlies the second. Although the first mechanism generally is accepted in principal, it is unclear whether the intermolecular interactions involved occur directly between the two receptors or whether intermediary proteins are required (Caswell and Brandt, 1989). The extent to which Ca^{2+}-induced Ca^{2+} release occurs in vertebrate skeletal muscle fibers is somewhat more controversial, and differing results have been obtained in different laboratories (e.g., Rios and Pizarro, 1988; Jacquemond et al., 1991; Jong et al., 1993). Recently, an additional complexity has been reported by Escobar et al. (1994), who found kinetic differences in the Ca^{2+} release transients recorded near the z- and m-lines within a single sarcomere in frog fast twitch skeletal muscle fibers. These results suggest that either spatially or mechanistically distinct processes are involved in activating SR Ca^{2+} release in these muscles.

If both mechanisms are utilized to activate SR Ca^{2+} release in situ, then an obvious possibility is that each of the two RyR isoforms in nonmammalian vertebrate skeletal muscles can be specialized to subserve one of the mechanisms. In this case, one isoform would be adapted for interactions with the dihydropyridine receptor, whereas the other would be more sensitive to activation by Ca^{2+}. The first isoform would share features with the RyR isoform expressed in mammalian skeletal muscles. In cardiac muscle, only a Ca^{2+}-induced Ca^{2+} release mechanism appears to activate SR Ca^{2+} release. Thus, if we make the assumption that the Ca^{2+}-induced Ca^{2+} release mechanisms are similar in skeletal and cardiac muscles, then the second chicken skeletal muscle RyR might be anticipated to have properties in common with the mammalian cardiac RyR isoform. Therefore, it is of interest to

compare the properties of the chicken skeletal muscle α- and βRyR receptors with those reported for the mammalian skeletal and cardiac muscle RyR isoforms.

The chicken α- and βRyRs do have a number of properties in common with the mammalian skeletal and cardiac muscle isoforms, respectively. The α- and mammalian skeletal muscle RyR isoforms both have relatively short openings and (at least under some conditions for the αRyR) both are relatively inactive in the presence of Ca^{2+} alone and are activated to relatively greater extents by adenine nucleotides than by Ca^{2+} (Smith et al., 1988). The chicken β and the mammalian cardiac muscle (Anderson et al., 1989; Rousseau et al., 1986) RyRs have similar properties in that both channels have longer openings, are activated at lower Ca^{2+} concentrations than the αRyR and the mammalian skeletal RyR channels, respectively, and both are activated to a greater relative extent by Ca^{2+} than by ATP. In addition, activation of both the β and the mammalian cardiac RyRs by Ca^{2+} occurs via an increase in the frequency of opening with relatively little effect on the duration of open events.

Although the preceding similarities provide circumstantial evidence for common physiological roles of the αRyR/mammalian skeletal muscle and βRyR/mammalian cardiac RyR pairs, the finding that perchlorate anions activate the α-, but not the β-, RyR isoform has more direct implications. As noted above, work from several laboratories has demonstrated the ability of perchlorate to enhance E-C coupling in skeletal muscle. This effect has been proposed to be specific for E-C coupling processes involving dihydropyridine receptor-RyR interactions (Rios et al, 1993). Consistent with this notion, perchlorate does not effect E-C coupling in mammalian cardiac (Ma et al., 1993) or barnacle muscle fibers (Gyorke and Palade, 1992), both of which utilize only the Ca^{2+}-induced Ca^{2+} release mechanism to activate SR Ca^{2+} release. In addition, perchlorate ions increased the activity of mammalian skeletal muscle RyR channels reconstituted in planar lipid bilayers, and this effect has been proposed to underlie the actions of the ions on muscle E-C coupling (Ma et al., 1993). Recently, perchlorate has been shown to act at the same site utilized by inorganic phosphate to influence the activity of the mammalian skeletal muscle RyR channel (Fruen et al., 1994a, b). Consistent with the lack of effect of perchlorate on E-C coupling in cardiac muscle, inorganic phosphate does not alter the behavior of the mammalian cardiac RyR (Fruen et al., 1994), suggesting that the cardiac receptor lacks the site affected by phosphate and perchlorate. The activation of α-, but not β-, RyR channels by perchlorate suggests that the αRyR can be positioned to interact with the dihydropyridine receptor. If this is the case, it would be predicted that perchlorate anions would enhance E-C coupling when the αRyR is expressed, e.g., in both embryonic and neonatal chick skeletal muscles (Sutko et al., 1991), but not when this isoform is absent, e.g., in *Crooked Neck Dwarf* (cn) mutant muscle cells (Airey et al., 1993a, b). We are currently working to test this prediction and to establish the effects of inorganic phosphate on the α- and βRyR channels.

The ability of positive potentials on the *cis* (cytoplasmic) side of the bilayer to inactivate both the α- and βRyR channels suggests an additional way in which the activity of these channels could be regulated in situ. The release of Ca^{2+} is not thought to cause a sustained electrical potential change across the SR membrane because of the presence of both chloride and potassium compensating currents (Meissner, 1988; Abramcheck and Best, 1989). The RyR channel inactivation observed at positive voltages was dependent on both voltage and time in an inverse manner. The greater the magnitude of the applied voltage, the shorter the interval before inactivation was observed (A. L. Percival, J. A. Airey, and J. L. Sutko, unpublished observations). With both channel isoforms, this activation involved the appearance of a very long-lived closed state, and in many cases the sign of the applied voltage had to be reversed before the channel would again open.

A voltage (and time)-dependent RyR inactivation could serve to regulate channel activity in a manner sensitive both to the quantity of Ca^{2+} released and the reestablishment of a normal level of Ca^{2+} (or of a compensating ionic charge) within the SR lumen. This could permit the release of a reproducible quantity of Ca^{2+} sufficient to activate fully, but not overload, the fiber in response to each excitation. The extent that the inactivation of SR Ca^{2+} release by Ca^{2+} involves or interacts with an associated Ca^{2+} diffusion potential remains to be determined. This aspect may be addressable by comparing the effects of voltage under conditions that result in the presence and absence of Ca^{2+}-dependent inhibition (e.g., on βRyR channels in millimolar *cis* Ca^{2+} ± ATP, see Fig. 6, *C* and *E*). Fill et al. (1989) reported a voltage-dependent gating of the mammalian skeletal muscle RyR channel. This involved channel inactivation at negative voltages that was observed at a pH of 7.2, but not at 7.4. Because of its dependence on pH and voltages of the opposite polarity, this appears to be a different phenomenon from that observed in our studies.

Channel activities identical to those observed for purified α- and βRyRs were found after fusion of native SR membranes with the bilayer. This was important because after purification the two isoforms have different physical properties, as indicated by the differences in the ease with which they could be incorporated into bilayers and in the effects of changes in detergent-lipid levels on [^{3}H]ryanodine binding. These results raised the possibility that some of the differences observed in the ion channel properties of the two isoforms could be attributed to varying responses to the solubilization and purification procedures. This does not appear to be the case, because similar differences in gating and in relative responses to activation by Ca^{2+} and ATP were observed when both purified proteins and native membranes were studied.

Recent evidence from several laboratories (Oyamada et al., 1994; V. Sorrentino, personal communication; J. A. Airey, unpublished observations) suggests that the βRyR expressed in frog and chicken skeletal muscles is most homologous to the mammalian RyR3 isoform. Therefore,

investigations of the former protein may provide insights into the functional properties of the latter isoform, which was cloned and sequenced from mammalian brain (Hakamata et al., 1992).

In conclusion, the α- and βRyR isoforms co-expressed in chicken skeletal muscles contain ryanodine-sensitive, Ca^{2+} release channels with similar conductance and selectivity characteristics. Previous studies have demonstrated the potential for differential regulation of the α- and βRyR channels, because these two proteins differ in the extents to which they are phosphorylated by Ca^{2+}-calmodulin-dependent and cAMP-dependent protein kinases and to which they bind calmodulin (Airey et al., 1993c). The present results demonstrate directly that the channels associated with each isoform differ in their gating properties and in their sensitivities to channel modifiers. Because of such differences, these proteins may have distinct roles in E-C coupling in chicken skeletal muscle. The differential expression of the isoforms in embryonic muscle (Sutko et al., 1991), the sustained expression of both isoforms in mature muscle (Airey et al., 1990), and the failure to develop normal E-C coupling in cn/cn muscle in the absence of normal αRyR protein (Airey et al., 1993a, b) suggest that the activity of each isoform is essential for the normal development of embryonic muscle and for mature muscle function.

The authors wish to thank Drs. Bill Welch and Andy Tinker for their critical comments on this manuscript and Drs. Robert Godt and Noel Davies for providing the programs used to calculate free Ca^{2+} levels.

This work was supported by National Institutes of Health grant HL27470. A. J. Williams received support from the Nuffield Foundation during the initial stages of this project.

REFERENCES

Abramcheck, C. W., and P. M. Best. 1989. Physiological role and selectivity of the in situ potassium channel of the sarcoplasmic reticulum in skinned frog skeletal muscle fibers. *J. Gen. Physiol.* 93:1–21.

Airey, J. A., M. D. Baring, C. F. Beck, Y. Chelliah, T. J. Deerinck, M. H. Ellisman, L. Houenou, D. D. McKemy, J. L. Sutko, and J. Talvenheimo. 1993a. A failure to make normal α ryanodine receptor is an early event associated with the Crooked Neck Dwarf (cn) mutation in chicken. *Dev. Dynam.* 197:169–188.

Airey, J. A., C. F. Beck, S. J. Tanksley, K. Murakami, T. J. Deerinck, M. H. Ellisman, and J. L. Sutko. 1990. Identification and localization of two triad junctional foot protein isoforms in mature avian fast twitch skeletal muscle. *J. Biol. Chem.* 265:14187–14194.

Airey, J. A., T. J. Deerinck, M. H. Ellisman, L. Houenou, A. Ivanenko, J. L. Kenyon, D. D. McKemy, and J. L. Sutko. 1993b. Crooked Neck Dwarf (cn) chicken skeletal muscle cells in low density cultures fail to express normal α ryanodine receptor and exhibit a partial mutant phenotype. *Dev. Dynam.* 197:189–202.

Airey, J. A., M. M. Grinsell, L. R. Jones, J. L. Sutko, and D. R. Witcher. 1993c. Three ryanodine receptor isoforms exist in avian striated muscles. *Biochemistry.* 32:5739–5745.

Anderson, K., F. A. Lai, Q.-Y. Liu, E. Rousseau, H. P. Erickson, and G. Meissner. 1989. Structural and functional characterization of the purified cardiac ryanodine receptor-Ca^{2+} release channel complex. *J. Biol. Chem.* 264:1329–1335.

Bull, R., and J. J. Marengo. 1993. Sarcoplasmic reticulum release channels from frog skeletal muscle display two types of calcium dependence. *FEBS Lett.* 331:223–227.

Campbell, K. P., C. M. Knudson, T. Imagawa, A. T. Leung, J. L. Sutko, S. D. Kahl, C. R. Raab, and L. Madson. 1987. Identification and characterization of the high affinity [^{3}H]ryanodine receptor of the junctional sarcoplasmic reticulum Ca^{2+} release channel. *J. Biol. Chem.* 262: 6460–6463.

Caswell, A. H., and N. R. Brandt. 1989. Does muscle activation occur by direct mechanical coupling of transverse tubules to sarcoplasmic reticulum? *Trends Biochem. Sci.* 14:161–165.

Colquhoun, D., and F. J. Sigworth. 1983. Fitting and statistical analysis of single-channel records. *In* Single Channel Recording. B. Sakmann and E. Neher, editors. Plenum Press, New York. 191–263.

Delcour, A. H., and R. W. Tsien. 1993. Altered prevalence of gating modes in neurotransmitter inhibition of N-type calcium channels. *Science.* 259: 980–984.

Escobar, A., J. Monck, J. Fernandez, and J. Vergara. 1994. Localization of the site of Ca^{2+} release at the level of a single sarcomere in skeletal muscle fibres. *Nature.* 367:739–741.

Fatt, P., and B. L. Ginsborg. 1958. The ionic requirements for the production of action potentials in crustacean muscle fibres. *J. Physiol. (Lond.).* 142: 516–543.

Fill, M., J. Ma, C. M. Knudson, T. Imagawa, K. P. Campbell, and R. Coronado. 1989. Role of the ryanodine receptor of skeletal muscle in excitation-contraction coupling. *Ann. N. Y. Acad. Sci.* 560: 155–162.

Fruen, B. R., J. R. Mickelson, N. H. Shomer, T. J. Roghair, and C. F. Louis. 1994a. Regulation of the sarcoplasmic reticulum ryanodine receptor by inorganic phosphate. *J. Biol. Chem.* 269:192–198.

Fruen, B. R., J. R. Mickelson, T. J. Roghair, H.-L. Cheng, and C. F. Louis. 1994b. Anions that potentiate E-C coupling may mimic effect of phosphate on calcium release channel. *Am. J. Physiol.* 266:C1729–C1735.

Gallant, E. M., N. S. Taus, T. F. Fletcher, L. R. Lentz, C. F. Louis, and J. R. Mickelson. 1993. Perchlorate potentiation of excitation-contraction coupling in mammalian skeletal muscles. *Am. J. Physiol.* 264:C559–C567.

Giannini, G., E. Clementi, R. Ceci, G. Marziali, and V. Sorrentino. 1992. Expression of a ryanodine receptor-Ca^{2+} channel that is regulated by TGF-β. *Science.* 257:91–94.

Gonzalez, A., and E. Rios. 1993. Perchlorate enhances transmission in skeletal muscle excitation-contraction coupling. *J. Gen. Physiol.* 102: 373–421.

Gyorke, S., and P. Palade. 1992. Effects of perchlorate on excitation-contraction coupling in frog and crayfish skeletal muscle. *J. Physiol. (Lond.).* 456:443–451.

Hakamata, Y., J. Nakai, H. Takeshima, and K. Imoto. 1992. Primary structure and distribution of a novel ryanodine receptor/calcium release channel from rabbit brain. *FEBS Lett.* 312:229–235.

Herrmann-Frank, A., and M. Varsanyi. 1993. Enhancement of Ca^{2+} release channel activity by phosphorylation of the skeletal muscle ryanodine receptor. *FEBS Lett.* 332:237–242.

Hess, P., J. B. Lansman, and R. W. Tsien. 1984. Different modes of Ca^{2+} channel gating behavior favoured by dihydropyridine Ca^{2+} agonists and antagonists. *Nature.* 311:538–544.

Hollingworth, S., A. B. Harkins, N. Kurebayashi, M. Konishi, and S. M. Baylor. 1992. Excitation-contraction coupling in intact frog skeletal muscle fibers injected with mmolar concentrations of fura-2. *Biophys. J.* 63:224–234.

Imagawa, T., J. S. Smith, R. Coronado, and K. P. Campbell. 1987. Purified ryanodine receptor from skeletal muscle sarcoplasmic reticulum is the Ca^{2+}-permeable pore of the calcium release channel. *J. Biol. Chem.* 262: 16636–16643.

Inui, M., A. Saito, and S. Fleischer. 1987. Purification of the ryanodine receptor and identity with feet structures of junctional terminal cisternae of sarcoplasmic reticulum from fast skeletal muscle. *J. Biol. Chem.* 262: 1740–1747.

Jacquemond, V., L. Csernoch, M. G. Klein, and M. F. Schneider. 1991. Voltage-gated and calcium-gated calcium release during depolarization of skeletal muscle fibers. *Biophys. J.* 60:867–873.

Jayaraman, T., A.-M. Brillantes, A. P. Timerman, S. Fleischer, H. Erdjument-Bromage, P. Tempst, and A. R. Marks. 1992. FK506 binding protein associated with the calcium release channel (ryanodine receptor). *J. Biol. Chem.* 267:9474–9477.

Jong, D.-S., P. C. Pape, W. K. Chandler, and S. M. Baylor. 1993. Reduction of calcium inactivation of sarcoplasmic reticulum calcium release by

fura-2 in voltage-clamped cut twitch fibers from frog muscle. *J. Gen. Physiol.* 102:333–370.

Lai, F. A., H. P. Erickson, E. Rousseau, Q.-Y. Liu, and G. Meissner. 1988. Purification and reconstitution of the calcium release channel from skeletal muscle. *Nature.* 331:315–319.

Lai, F. A., Q.-Y. Liu, L. Xu, A. El-Hashem, N. R. Kramarcy, R. Sealock, and G. Meissner. 1992. Amphibian ryanodine receptor isoforms are related to those of mammalian skeletal or cardiac muscle. *Am. J. Physiol.* 263:C365–C372.

Lindsay, A. R. G., S. D. Manning, and A. J. Williams. 1991. Monovalent cation conductance in the ryanodine receptor-channel of sheep cardiac muscle sarcoplasmic reticulum. *J. Physiol. (Lond.).* 439:463–480.

Lindsay, A. R. G., and A. J. Williams. 1991. Functional characterization of the ryanodine receptor purified from sheep cardiac muscle sarcoplasmic reticulum. *Biochim. Biophys. Acta.* 1064:89–102.

Lowry, O. H., N. J. Rosebrough, A. L. Farr, and R. J. Randall. 1951. Protein measurement with the Folin phenol reagent. *J. Biol. Chem.* 193:265–275.

Ma, J., K. Anderson, R. Ahirokov, R. Levis, A. Gonzalez, M. Karhanek, M. M. Hosey, G. Meissner, and E. Rios. 1993. Effects of perchlorate on the molecules of excitation-contraction coupling of skeletal and cardiac muscle. *J. Gen. Physiol.* 102:423–448.

Meissner, G. 1988. Ionic permeability of isolated muscle sarcoplasmic reticulum and liver endoplasmic reticulum vesicles. *Methods Enzymol.* 157: 417–437.

Meissner, G., E. Rousseau, and F. A. Lai. 1989. Structural and functional correlation of the trypsin-digested Ca^{2+} release channel of skeletal muscle sarcoplasmic reticulum. *J. Biol. Chem.* 264:1715–1722.

Murayama, T., and Y. Ogawa. 1992. Purification and characterization of two ryanodine-binding protein isoforms from sarcoplasmic reticulum of bullfrog skeletal muscle. *J. Biochem.* 112:514–522.

Nowycky, M. C., A. P. Fox, and R. W. Tsien. 1985. Long-opening mode of gating of neuronal calcium channels and its promotion by the dihydropyridine calcium agonist Bay K 8644. *Proc. Natl. Acad. Sci. USA.* 82:2178–2182.

O'Brien, J., G. Meissner, and B. A. Block. 1993. The fastest contracting muscles of nonmammalian vertebrates express only one isoform of the ryanodine receptor. *Biophys. J.* 65:2418–2427.

Olivares, E., S. J. Tanksley, J. A. Airey, C. F. Beck, T. J. Deerinck, M. H. Ellisman, and J. L. Sutko. 1991. Multiple foot protein isoforms in amphibian, avian and piscine skeletal muscles. *Biophys. J.* 59: 1153–1163.

Oyamada, H., T. Murayama, T. Takagi, M. Iino, N. Iwabe, T. Miyata, Y. Ogawa, and M. Endo. 1994. Primary structure and distribution of ryanodine-binding protein isoforms of the bullfrog skeletal muscle. *J. Biol. Chem.* 269:17206–17214.

Pape, P. C., D.-S. Jong, W. K. Chandler, and S. M. Baylor. 1993. Effect of fura-2 on action potential-stimulated calcium release in cut twitch fibers from frog muscle. *J. Gen. Physiol.* 102:295–332.

Peterson, G. L. 1977. A simplification of the protein assay of Lowry et al. which is more generally applicable. *Anal. Biochem.* 83:346–356.

Rios, E., M. Karhanek, J. Ma, and A. Gonzalez. 1993. An allosteric model of the molecular interactions of excitation-contraction coupling in skeletal muscle. *J. Gen. Physiol.* 102:449–481.

Rios, E., and G. Pizarro. 1988. Voltage sensors and calcium channels of excitation-contraction coupling in skeletal muscle. *News Physiol. Sci.* 3:223–227.

Rios, E., and G. Pizarro. 1991. Voltage sensor of excitation-contraction coupling in skeletal muscle. *Physiol. Rev.* 71:849–908.

Rousseau, E., J. LaDine, Q.-Y. Liu, and G. Meissner. 1988. Activation of the Ca^{2+} release channel of skeletal muscle sarcoplasmic reticulum by caffeine and related compounds. *Arch. Biochem. Biophys.* 267: 75–86.

Rousseau, E., and G. Meissner. 1989. Single cardiac sarcoplasmic reticulum Ca^{2+}-release channel: activation by caffeine. *Am. J. Physiol.* 256: H328–H333.

Rousseau, E., J. S. Smith, J. S. Henderson, and G. Meissner. 1986. Single channel and $^{45}Ca^{2+}$ flux measurements of the cardiac sarcoplasmic reticulum calcium channel. *Biophys. J.* 50:1009–1014.

Rousseau, E., J. S. Smith, and G. Meissner. 1987. Ryanodine modifies conductance and gating behavior of single Ca^{2+} release channel. *Am. J. Physiol.* 253:C364–C368.

Sanchez, J. A., and J. Vergara. 1994. Modulation of Ca^{2+} transients by photorelease of caged nucleotides in frog skeletal muscle fibers. *Am. J. Physiol.* 266:C1291–C1300.

Simon, B. J., M. G. Klein, and M. F. Schneider. 1991. Calcium dependence of inactivation of calcium release from the sarcoplasmic reticulum in skeletal muscle fibers. *J. Gen. Physiol.* 97:437–471.

Smith, J. S., R. Coronado, and G. Meissner. 1985. Sarcoplasmic reticulum contains adenine nucleotide-activated calcium channels. *Nature.* 316:446–449.

Smith, J. S., R. Coronado, and G. Meissner. 1986. Single-channel calcium and barium currents of large and small conductance from sarcoplasmic reticulum. *Biophys. J.* 50:921–928.

Smith, J. S., T. Imagawa, J. Ma, M. Fill, K. P. Campbell, and R. Coronado. 1988. Purified ryanodine receptor from rabbit skeletal muscle is the calcium-release channel of sarcoplasmic reticulum. *J. Gen. Physiol.* 92: 1–26.

Suarez-Isla, B. A., C. Alcayaga, J. J. Marengo, and R. Bull. 1991. Activation of inositol trisphosphate-sensitive Ca^{2+} channels of sarcoplasmic reticulum from frog skeletal muscle. *J. Physiol.* 441:575–591.

Sutko, J. L., J. A. Airey, K. Murakami, C. F. Beck, S. Tanksley, M. Takeda, T. J. Deerinck, and M. H. Ellisman. 1991. Expression of α and β foot protein isoforms during embryonic development of avian skeletal muscle. *J. Cell Biol.* 113:793–803.

Takasago, T., T. Imagawa, K. Furukawa, T. Ogurusu, and M. Shigekawa. 1991. Regulation of the cardiac ryanodine receptor by protein kinase-dependent phosphorylation. *J. Biochem. (Tokyo).* 109:163–170.

Timerman, A. P., E. Ogunbumni, E. Freund, G. Wiederrecht, A. R. Marks, and S. Fleischer. 1993. The calcium release channel of sarcoplasmic reticulum is modulated by FK-506-binding protein. *J. Biol. Chem.* 268: 22992–22999.

Wang, J., and P. M. Best. 1992. Inactivation of the sarcoplasmic reticulum calcium channel by protein kinase. *Nature.* 359:739–741.

Williams, A. J. 1992. Ion conduction and discrimination in the sarcoplasmic reticulum ryanodine receptor/calcium-release channel. *J. Muscle Res. Cell Motil.* 13:7–26.

Witcher, D. R., R. J. Kovacs, H. Schulman, D. C. Cefali, and L. R. Jones. 1991. Unique phosphorylation site on the cardiac ryanodine receptor regulates calcium channel activity. *J. Biol. Chem.* 266:11144–11152.

Yoshida, A., M. Takahashi, T. Imagawa, M. Shigekawa, H. Takisawa, and T. Nakamura. 1992. Phosphorylation of ryanodine receptors in rat myocytes during β-adrenergic stimulation. *J. Biochem. (Tokyo)* 111:186–190.